Bootstrapping Laplace Transforms of Volatility

Hounyo, Ulrich; Liu, Zhi; Varneskov, Rasmus T.

Document Version
Final published version

Published in:
Quantitative Economics

DOI:
10.3982/QE1929

Publication date:
2023

Quantitative Economics 14 (2023), 1059–1103 1759-7331/20231059

Bootstrapping Laplace transforms of volatility

Ulrich Hounyo
Department of Economics, University at Albany—State University of New York

Zhi Liu
Department of Mathematics, University of Macau

Rasmus T. Varneskov
Department of Finance, Copenhagen Business School and Multi Assets, Nordea Asset Management

This paper studies inference for the realized Laplace transform (RLT) of volatility in a fixed-span setting using bootstrap methods. Specifically, since standard wild bootstrap procedures deliver inconsistent inference, we propose a local Gaussian (LG) bootstrap, establish its first-order asymptotic validity, and use Edgeworth expansions to show that the LG bootstrap inference achieves second-order asymptotic refinements. Moreover, we provide new Laplace transform-based estimators of the spot variance as well as the covariance, correlation, and beta between two semimartingales, and adapt our bootstrap procedure to the requisite scenario. We establish central limit theory for our estimators and first-order asymptotic validity of their associated bootstrap methods. Simulations demonstrate that the LG bootstrap outperforms existing feasible inference theory and wild bootstrap procedures in finite samples. Finally, we illustrate the use of the new methods by examining the coherence between stocks and bonds during the global financial crisis of 2008 as well as the COVID-19 pandemic stock sell-off during 2020, and by a forecasting exercise.

Keywords. Bootstrap, Edgeworth expansions, high-frequency data, higher-order refinements, Itô semimartingales, realized Laplace transform, spot measure inference.

JEL classification. C14, C15, G1.

1. Introduction

Stochastic volatility is a distinct feature of many economic and financial time series, and has significant implications for asset and derivatives pricing, risk management, portfolio selection, among others. In fact, the importance of accounting for such dependencies

Ulrich Hounyo: khounyo@albany.edu
Zhi Liu: liuzhi@um.edu.mo
Rasmus T. Varneskov: rtv.fi@cbs.dk

We thank two anonymous referees, Prosper Dovonon, and Viktor Todorov for helpful comments. Hounyo and Varneskov gratefully acknowledge financial support from CREATES, Center for Research in Econometric Analysis of Time Series (DNRF78), funded by the Danish National Research Foundation, and Varneskov from the Danish Finance Institute (DFI). Liu's research is partially supported by NSFC (No. 11971507) and the Science and Technology Development Fund, Macau SAR (File no. 0041/2021/ITP).

 https://doi.org/10.3982/QE1929

in economic decision-making has been firmly recognized for, at least, two decades, for example, Engle (2004). While inference for models of stochastic volatility is inherently difficult since the underlying volatility process is latent, the recent availability of high-frequency financial data has allowed researchers to aggregate observations into specific measures of volatility, aiding in the recovery of information about its underlying dynamics.

The realized variance, defined as the sum of squared intraday returns, is a prominent example of a volatility measure, representing a nonparametric estimate of the unobserved quadratic variation over a fixed time period; see, for example, Andersen, Bollerslev, Diebold, and Labys (2001, 2003) and Barndorff-Nielsen and Shephard (2002). Since its introduction, the scope and use of high-frequency data have been significantly broadened, leading to jump-robust measures of integrated variance and jump tests, for example, Barndorff-Nielsen and Shephard (2004b), Aït-Sahalia and Jacod (2009), Mancini (2009); multivariate measures of the quadratic covariation between assets, for example, Barndorff-Nielsen and Shephard (2004a) and Hayashi and Yoshida (2005); measures that are robust to market microstructure frictions, for example, Zhang, Mykland, and Aït-Sahalia (2005), Barndorff-Nielsen, Hansen, Lunde, and Shephard (2008), and Jacod, Li, Mykland, Podolskij, and Vetter (2009); and measures that tackle all three features and leverage them to study various problems in economics and finance, see, for example, Andersen, Bollerslev, Christoffersen, and Diebold (2013), Aït-Sahalia and Jacod (2014), Varneskov (2017), and many references therein.

The realized Laplace transform (RLT), defined as the simple average of cosine transforms for (appropriately rescaled) high-frequency increments, represents an important alternative volatility measure. It captures the empirical Laplace transform of the spot variance process over a fixed interval of time, thus preserving information about the characteristics of volatility. Since its introduction by Todorov and Tauchen (2012b), the RLT has been utilized, among others, to design estimation procedures for stochastic volatility models, for example, Todorov, Tauchen, and Grynkiv (2011); volatility density estimation, Todorov and Tauchen (2012a); inference procedures and tests for the jump activity index, Todorov (2015); estimation of option pricing models, Andersen, Fusari, Todorov, and Varneskov (2019). These methods, however, generally use fixed-span estimates of the RLT as ingredients in long-span inference procedures (Andersen et al. (2019) use a large option cross-section), imposing stationarity and mixing-type conditions on the volatility. Such conditions may be reasonable for analyzing data over very long sample periods, but are unlikely to describe the volatility process well for shorter samples where the latter may be highly persistent and exhibit outright nonstationarities, for example, Comte and Renault (1998). Similarly, Casini and Perron (2019) design Laplace-based inference for structural change models using continuous record asymptotics in a setting with joint infill and long-span asymptotics.

At present, little is known about the quality of inference using RLT measures over fixed time spans. This paper fills this gap. Specifically, in an infill asymptotic setting, we study bootstrap inference procedures for the RLT, allowing the volatility to be very persistent and nonstationary. Interestingly, despite the RLT having features suggesting that a wild bootstrap may be appropriate, such as its summands being uncorrelated and heteroskedastic, we show that the variants provided by Wu (1986) and Liu (1988) as well as Gonçalves and Meddahi (2009), in different contexts deliver inconsistent inference in the present setting. As a solution, we propose a local Gaussian (LG) bootstrap procedure and establish its first-order asymptotic validity in a general semimartingale framework. Moreover, motivated by its excellent finite sample performance in our numerical analysis, we further study the higher-order properties of the LG bootstrap procedure using Edgeworth expansions in a simplified dynamic setting, ruling out drift, jumps, and leverage effects (as for the equivalent analyses in Gonçalves and Meddahi (2009) and Dovonon, Gonçalves, Hounyo, and Meddahi (2019)), and show that it is capable of delivering second-order refinements over the standard Gaussian approximation. Importantly, we maintain a general semimartingale assumption for volatility when deriving the higher-order results, unlike existing references who impose additional smoothness, for example, Hölder continuity.

We broaden the scope, and thus applications, of the RLT and our LG bootstrap approach by providing inference procedures for the spot Laplace transform (SLT). These are then used to design new Laplace-based estimators and associated bootstrap inference procedures for the spot variance as well as the spot covariance, correlation, and beta between two semimartingale processes. The estimators achieve the optimal rate of convergence $\Delta_n^{-1/4}$, with Δ_n being the mesh between observations. Moreover, first-order asymptotic validity of the LG bootstrap methods is established at a near-optimal rate, and our higher-order Edgeworth expansion analysis suggests that the LG bootstrap offers very accurate inference. The theoretical findings are confirmed in a simulation study where the latter provide substantial improvements in coverage rates for the RLT as well as the spot variance, covariance, correlation, and beta between two assets compared with alternative inference procedures based on feasible limit theory, existing (inconsistent) wild bootstrap methods, and a modified wild bootstrap, which is analyzed theoretically in a companion note to this paper (Hounyo, Liu, and Varneskov (2022)).

The attractive properties of the new LG bootstrap procedure for the RLT and our SLT-based estimators of the spot variance, covariance, correlation, and beta may readily be leveraged to design fixed span inference for stochastic volatility models, volatility densities, jump activity indices, option-pricing models, and structural break tests, as referenced above. Furthermore, they may provide equally useful ingredients for inference procedures that depend on the spot volatility matrix such as volatility functionals and functional dependencies, Jacod and Rosenbaum (2013), Li, Todorov, and Tauchen (2016), and Li, Liu, and Xiu (2019); GMM estimation involving moments that depend on volatility, Li and Xiu (2016); and for carrying out tests for jumps and jump arrival times, Lee and Mykland (2008).

We illustrate the usefulness of our spot measures and bootstrap inference procedures for risk management by providing estimates and confidence intervals for the spot volatilities of the S&P 500 and 10-year US Treasury bonds as well as their spot correlation and (market) beta from January 2005 through December 2020. Specifically, we show that bonds have provided an effective equity hedge during the global financial crisis in 2008, but lacked protective ability during the COVID-19 pandemic stock sell-off in 2020, thus revealing an anatomy of two different crisis. Hence, by leveraging our precise fixed-span bootstrap inference procedures, our results show that static stock-bond portfolios have enjoyed substantial diversification benefits during 2008 and have suffered from a lack of fixed income protection during 2020, thereby calling for a dynamic approach to balanced portfolio construction. Finally, our (bootstrap) methods provide useful information for risk measure forecasting.

This paper adds to a growing literature on bootstrap inference for statistics based on realized measures using high-frequency data; see, for example, Gonçalves and Meddahi (2009), Hounyo, Gonçalves, and Meddahi (2017), Hounyo (2017, 2019), Hounyo and Varneskov (2017), and Dovonon et al. (2019). In those studies, the bootstrap procedures are developed for realized volatility-style measures, whereas in this paper we consider bootstrap inference for the RLT and for statistics based on smooth transformations of the *spot* covariance between two semi-martingale processes. As carefully explained on Todorov and Tauchen (2012b, p. 1106), the main difference between realized volatility measures and the RLT is that the latter is a mapping from the data to a *random process*, while realized volatility measures are simple mappings from the data to *random variables*. Hence, our bootstrap inference procedure has to accommodate the nonlinear cosine transform of high-frequency increments in the design, and we need to provide both pointwise and uniform limit theory for the bootstrap to remain valid over the entire space of the random (Laplace) function. Not only does this add substantial complexity to the first-order asymptotic analysis, it makes the higher-order analysis particularly novel. In fact, this paper is the first to even provide first-order uniform functional limit theory for bootstrap inference on a continuous and bounded function in the high-frequency econometrics literature. The uniform results are necessary for the design of, and inference for, our spot (co)variance estimators, which are constructed by transforming the SLT and evaluating it over a compact support.

The paper also adds to the literature on spot (co)variance estimation, which dates back to Foster and Nelson (1996) and Comte and Renault (1998), and has recently seen a surge in interest with new nonparametric estimators being introduced in semimartingale settings by, among others, Lee and Mykland (2008), Aït-Sahalia and Jacod (2009), Kristensen (2010), Bandi and Reno (2016, 2018); and when the observations are contaminated with market microstructure noise by, for example, Zu and Boswijk (2014) and Bibinger, Hautsch, Malec, and Reiss (2019). Specifically, we provide new jump-robust spot (co)variance estimators and associated bootstrap inference based on a kernel-weighted Laplace transform. Importantly, we show that our estimators enjoy smaller finite sample bias and lower mean squared errors than the popular truncated local realized volatility estimator in our simulation study.

The rest of the paper is organized as follows. In Section 2, we provide the framework, state assumptions, and introduce the statistics of interest. Section 3 studies first-order validity of LG bootstrap inference for the RLT. Moreover, Section 4 has results on second-order expansions for the cumulants of the original t-statistic as well as their bootstrap analogs and shows that the LG bootstrap achieves asymptotic refinements. Section 5 provides the SLT as well as estimators of the spot (co)variance and associated bootstrap inference. While Section 6 has Monte Carlo simulations, Section 7 illustrates the use of the new estimators and inference procedures in an empirical exercise. Finally, Section 8 concludes. The Appendix provides additional assumptions and study the properties of existing wild bootstrap methods. The Online Supplementary Appendix (Hounyo, Liu, and Varneskov (2023)) contains all proofs.

2. Setup, assumptions, and first-order asymptotic theory

This section introduces the setup and states the formal assumptions. Moreover, we define the statistics of interest for the bootstrap analysis in the remainder of the paper.

2.1 *Setup and assumptions*

Suppose the process X is defined on a filtered probability space, $(\Omega, \mathcal{F}, (\mathcal{F}_t), \mathbb{P})$, where the information filtration $(\mathcal{F}_t) \subseteq \mathcal{F}$ is an increasing family of σ-fields satisfying $\mathbb{P}$-completeness and right continuity. Specifically, assume that X obeys an Itô semimartingale with stochastic differential equation of the form,

$$dX_t = \alpha_t\,dt + \sigma_t\,dW_t + \int_{\mathbb{R}} \delta(t-, x)\mu(dt, dx), \tag{1}$$

where the drift α_t and volatility σ_t are $(\mathcal{F}_t)$-adapted processes with càdlàg paths, W_t is a standard Brownian motion, μ is a homogeneous Poisson measure with compensator $dt \otimes \nu(dx)$, ν is the Lévy measure, and $\delta(t, x) : \mathbb{R}_+ \times \mathbb{R} \to \mathbb{R}$ is càdlàg in t, where we let $\mathbb{R}_+ = \{x \in \mathbb{R} : x \geq 0\}$. For the theoretical analysis, we follow Todorov and Tauchen (2012b) and impose the following (mild) structure for the Lévy and stochastic volatility components of the process.

Assumption A. The Lévy measure ν satisfies

$$\mathbb{E}\left(\int_0^t \int_{\mathbb{R}} \left(\left|\delta(s, x)\right|^p \vee \left|\delta(s, x)\right|\right) ds\nu(dx)\right) < \infty,$$

for every $t > 0$ and every $p \in (\beta, 1)$, where $0 \leq \beta < 1$ is some constant.

Assumption B. The volatility, σ_t, is an Itô semimartingale, defined by

$$\sigma_t = \sigma_0 + \int_0^t \tilde{a}_s\,ds + \int_0^t v_s\,dW_s + \int_0^t v'_s\,dW'_s + \int_0^t \int_{\mathbb{R}} \delta'(s-, x)\tilde{\mu}'(ds, dx),$$

where W'_t is a Brownian motion, independent of W_t, $\tilde{\mu}'$ is a compensated homogeneous Poisson measure with Lévy measure $dt \otimes \nu'(dx)$, having arbitrary dependence with μ, and $\delta'(t, x) : \mathbb{R}_+ \times \mathbb{R} \to \mathbb{R}$ is càdlàg in t. In addition, for every $t, s > 0$ and some $\iota > 0$, it is required that

$$\mathbb{E}\left(|a_s|^{3+\iota} + |\tilde{a}_s|^2 + |\sigma_t|^{3+\iota} + |v_t|^{3+\iota} + \left|v'_t\right|^{3+\iota} + \int_{\mathbb{R}} \left|\delta'(t, x)\right|^{3+\iota} \nu'(dx)\right) < C,$$

$$\mathbb{E}\left(|a_t - a_s|^2 + |v_t - v_s|^2 + \left|v'_t - v'_s\right|^2 + \int_{\mathbb{R}} \left(\delta'(t, x) - \delta'(s, x)\right)^2 \nu'(dx)\right) < C|t - s|,$$

where $C > 0$ is some constant that is free of t and s.

Assumption A restricts the jump component of the model (1) to be of finite variation. However, since the activity index may vary in the range $0 \le \beta < 1$, its dynamics retain substantial flexibility, accommodating, for example, tempered stable processes as well as compound Poisson processes, which have activity index $\beta = 0$. Assumption B allows the stochastic volatility to be comprised of multiple factors and accommodates leverage effects between dX_t and $d\sigma_t$, working either through continuous or discontinuous, that is, jump, channels, whose magnitude and dynamics may differ substantially, for example, Aït-Sahalia, Fan, Laeven, Wang, and Yang (2017). Taken together, the setting covers most parametric jump-diffusion models in financial econometrics; see, for example, Andersen and Benzoni (2012).

Finally, we assume that T is fixed and, within the interval $[0, T]$, we observe the process X at the equidistant time points $\{0, \Delta_n, 2\Delta_n, \dots, i\Delta_n, \dots, n\Delta_n \equiv T\}$.

2.2 *The realized Laplace transform and its asymptotic theory revisited*

First, define $\Delta_i^n X \equiv X_{i\Delta_n} - X_{(i-1)\Delta_n}$ and $\xi(X, T, u)_i^n \equiv \cos(\sqrt{2u}\Delta_n^{-1/2}\Delta_i^n X)$, for some $u \ge 0$, then Todorov and Tauchen (2012b) introduces the realized Laplace transform (RLT) of volatility,

$$\mathrm{RLT}_n(X, T, u) = \Delta_n \sum_{i=1}^{n} \xi(X, T, u)_i^n, \tag{2}$$

for which $\mathrm{RLT}_n(u) \equiv \mathrm{RLT}_n(X, T, u)$ and $\xi(u)_i^n \equiv \xi(X, T, u)_i^n$ will be used as shorthand notation henceforth, despite being defined with respect to X and T. Moreover, on the space of continuous functions, $C(\mathbb{R}_+)$, indexed by u and equipped with the local uniform topology, Todorov and Tauchen (2012b, Theorem 1) provide *stable* central limit theory under Assumptions A and B,

$$\mathcal{S}_n(u) \equiv \Delta_n^{-1/2}\left(\mathrm{RLT}_n(u) - \int_0^T e^{-uc_s}\, ds\right) \xrightarrow{d_s} \Psi_T(u), \quad \text{as } \Delta_n \to 0, \tag{3}$$

where $c_t \equiv \sigma_t^2$ is the spot variance. The limiting process $\Psi_T(u)$ is defined on an extension of the original probability space, is $\mathcal{F}$-conditionally Gaussian, and is defined with a zero mean function and a covariance function given by $\int_0^T F(\sqrt{uc_s}, \sqrt{vc_s})\, ds$ for every $u, v \in \mathbb{R}_+$, where

$$F(x, y) = \frac{e^{-(x+y)^2} - 2e^{-x^2-y^2} + e^{-(x-y)^2}}{2}, \quad \text{for } x, y \in \mathbb{R}_+. \tag{4}$$

In addition to the asymptotic central limit theory, Todorov and Tauchen (2012b) provide a consistent estimator of $\int_0^T F(\sqrt{uc_s}, \sqrt{vc_s})\, ds$, defined as $\bar{C}_n(u, v) \equiv \Delta_n \sum_{i=1}^{\lfloor T/\Delta_n \rfloor} (\xi(u)_i^n \times \xi(v)_i^n - \xi(u+v)_i^n)$, thus facilitating feasible inference on the RLT. This estimator, however, is not guaranteed to be nonnegative when $u = v$ and we thus propose to replace it with an alternative nonnegative one,

$$\widehat{C}_n(u, v) \equiv \frac{\Delta_n}{2} \sum_{i=1}^{n-1} \big(\xi(u)_i^n - \xi(u)_{i+1}^n\big)\big(\xi(v)_i^n - \xi(v)_{i+1}^n\big), \quad u, v > 0, \tag{5}$$

where we, as above, have suppressed dependence on T and X from the notation.

PROPOSITION 1. *Suppose Assumptions A and B hold. Then, for any fixed $u, v > 0$, as $\Delta_n \to 0$,*

$$\widehat{C}_n(u, v) \xrightarrow{\mathbb{P}} \int_0^T F(\sqrt{uc_s}, \sqrt{vc_s})\, ds.$$

Hence, by combining the asymptotic results in (3) and Proposition 1, we obtain an alternative feasible inference limit theory for the RLT. Specifically, under Assumptions A and B, as $\Delta_n \to 0$,

$$T_n(u) \equiv \frac{\Delta_n^{-1/2}\left(\mathrm{RLT}_n(u) - \int_0^T e^{-uc_s}\, ds\right)}{\sqrt{\widehat{C}_n(u, u)}} \xrightarrow{d} N(0, 1), \tag{6}$$

which may be used to generate standard two-sided confidence intervals.

3. Bootstrap inference for the realized Laplace transform

It is important to stress that the volatility of (1) is stochastic under Assumption B. This implies that, conditional on the paths of the drift, volatility, and jump components of (1), the sequence $(\xi(u)_i^n)_{i=1}^n$ is uncorrelated and heteroskedastic, which, traditionally, motivate the use of a wild bootstrap procedures for drawing inference. However, in Appendix C, we demonstrate that the adaptations of two existing wild bootstrap procedures to the present setting; namely, those introduced by Gonçalves and Meddahi (2009) as well as Wu (1986) and Liu (1988) in different contexts, result in inconsistent inference for the RLT. Hence, this section proposes a new bootstrap inference procedure based on local Gaussian resampling and establish its first-order asymptotic validity. In particular, we demonstrate how it may be used to consistently estimate the distributions of $\mathcal{S}_n(u)$ in (3) and $T_n(u)$ in (6).

3.1 *Bootstrap notation*

As usual in the bootstrap inference literature, $\mathbb{P}^*$, $\mathbb{E}^*$, and $\mathbb{V}^*$ denote the probability measure, expected value and variance, respectively, induced by the resampling and is thus conditional on a realization of the original time series. For any bootstrap statistic $Z_n^* \equiv Z_n^*(\cdot, \omega)$ and any (measurable) set A, we write $\mathbb{P}^*(Z_n^* \in A) = \mathbb{P}^*(Z_n^*(\cdot, \omega) \in A) = \Pr(Z_n^*(\cdot, \omega) \in A | \mathcal{X}_n)$, where $\mathcal{X}_n$ denotes the observed sample. Moreover, we say $Z_n^* \xrightarrow{\mathbb{P}^*} 0$ in probability-$\mathbb{P}$ (or $Z_n^* = o_p^*(1)$ in probability-$\mathbb{P}$) if for any $\varepsilon > 0$, $\delta > 0$, $\lim_{n\to\infty} \mathbb{P}[\mathbb{P}^*(|Z_n^*| > \delta) > \varepsilon] = 0$. Similarly, $Z_n^* = O_p^*(1)$ in probability-$\mathbb{P}$ if for all $\varepsilon > 0$ there exists an $M_\varepsilon < \infty$ such that $\lim_{n\to\infty} \mathbb{P}[\mathbb{P}^*(|Z_n^*| > M_\varepsilon) > \varepsilon] = 0$. Finally, for a sequence of random variables (or vectors) Z_n^*, a definition of convergence in distribution in probability-$\mathbb{P}$ is needed.

DEFINITION 1. The statement $Z_n^* \xrightarrow{d^*} Z$ in probability-$\mathbb{P}$, as $n \to \infty$, signifies that $\mathbb{E}^*(f(Z_n^*)) \to \mathbb{E}(f(Z))$ in probability-$\mathbb{P}$ for every continuous and bounded function f.

Let $l^{\infty}(\mathbb{K})$ denote the space of bounded real-valued functions on a compact subset $\mathbb{K} \subset \mathbb{R}_+$, equipped with the supremum norm $\sup_{u \in \mathbb{K}} |z(u)|$, for some $z(u)$. Then, as for random variables, we need a definition of weak convergence for a sequence of random processes $Z_n^*(u)$ on $l^{\infty}(\mathbb{K})$ in probability-$\mathbb{P}$.

Definition 2. $Z_n^*(u) \overset{d^*}{\Longrightarrow} Z(u)$ on $l^{\infty}(\mathbb{K})$ in probability-$\mathbb{P}$ as $n \to \infty$ signifies that the sequence has $\sup_{h \in \mathbb{BL}_1(l^{\infty}(\mathbb{K}))} |\mathbb{E}^*(h(Z_n^*)) - \mathbb{E}(h(Z))| \overset{\mathbb{P}}{\to} 0$ where $\mathbb{BL}_1(l^{\infty}(\mathbb{K}))$ is the space of functions h: $l^{\infty}(\mathbb{K}) \to \mathbb{R}$ with Lipschitz norm bounded by 1, that is, for any $h \in \mathbb{BL}_1(l^{\infty}(\mathbb{K}))$, $\sup_{z \in l^{\infty}(\mathbb{K})} |h(z)| \leq 1$, and $|h(z_1) - h(z_2)| \leq d(z_1, z_2)$ for all z_1, z_2 in $l^{\infty}(\mathbb{K})$, where $d(z_1, z_2) = \sup_{u \in \mathbb{K}} |z_1(u) - z_2(u)|$.

Remark 1. The definition of weak convergence of a random process $Z_n^*(u)$ on $l^{\infty}(\mathbb{K})$ in probability-$\mathbb{P}$ is equivalent to saying that $\mathbb{E}^*(h(Z_n^*)) \to \mathbb{E}(h(Z))$ in probability-$\mathbb{P}$ for any $h : l^{\infty}(\mathbb{K}) \to \mathbb{R}$ and which is continuous and bounded with respect to the supremum norm.

In addition to bootstrap convergence modes and expectation operators, let $(\xi(u)_i^{n*})_{i=1}^n$ be a bootstrap sample constructed or obtained from $(\xi(u)_i^n)_{i=1}^n$. Moreover, let $\eta_1^*, \ldots, \eta_n^*$ be i.i.d. random variables, whose distribution is independent of the original sample and denote by $\mu_q^* \equiv \mathbb{E}^*((\eta_i^*)^q)$ its qth moment. Finally, we define the corresponding bootstrap RLT statistic as

$$\mathrm{RLT}_n^*(u) \equiv \Delta_n \sum_{i=1}^n \xi(u)_i^{n*}, \qquad \mathcal{S}_n^*(u) \equiv \Delta_n^{-1/2}\big(\mathrm{RLT}_n^*(u) - \mathbb{E}^*\big(\mathrm{RLT}_n^*(u)\big)\big), \tag{7}$$

along with its bootstrap covariance matrix as

$$C_n^*(u, v) \equiv \mathrm{Cov}^*\big(\Delta_n^{-1/2}\,\mathrm{RLT}_n^*(u), \Delta_n^{-1/2}\,\mathrm{RLT}_n^*(v)\big). \tag{8}$$

3.2 *The local Gaussian bootstrap for the RLT*

In this section, we propose a new bootstrap inference procedure for the RLT of volatility. Specifically, motivated by Dovonon et al. (2019) and Hounyo (2019), who show that local Gaussian resampling leads to favorable inference properties for the realized volatility measure, realized beta, and for jump tests, we generate bootstrap high-frequency increments $\Delta_i^n X^*$ as follows:

$$\Delta_i^n X^* = \sqrt{\Delta_n \hat{c}_i^n} \cdot \eta_i^*, \quad i = 1, \ldots, n, \tag{9}$$

for some (local) variance measure $\hat{c}_i^n$ that is based on $\{\Delta_i^n X : i = 1, \ldots, n\}$ and is defined below, and where η_i^* is generated independently of the data as $\eta_i^* \sim$ i.i.d. $N(0, 1)$. Consequently, we have

$$\xi(u)_i^{n*} = \cos\Big(\sqrt{2u\hat{c}_i^n}\,\eta_i^*\Big), \quad i = 1, \ldots, n. \tag{10}$$

That is, rather than resample the sequence $(\xi(u)_i^n)_{i=1}^n$, as for the wild bootstrap, we mimic the local dependence properties of the original increments, $\Delta_i^n X$, as $\Delta_n \to 0$ when constructing the bootstrap observations in (9), and subsequently apply the cosine transformation. Hence, relative to the analyses in Dovonon et al. (2019) and Hounyo (2019), we consider a nonlinear transformation of the local Gaussian bootstrap observations *and* study both pointwise as well as uniform (in u) central limit theory since the RLT constitutes a *random process* rather than a *random variable*.

Next, recall that $\mathbb{E}^*(e^{\mathrm{i}u\eta^*}) = e^{-u^2/2}$ for $\mathrm{i} = \sqrt{-1}$, $u \in \mathbb{R}$, and $\eta^* \sim N(0,1)$. Hence, $\mathbb{E}^*(\xi(u)_i^{n*}) = e^{-u\hat{c}_i^n}$ for observations $i = 1, \dots, n$, and, as a result, we may write

$$\mathbb{E}^*\big(\mathrm{RLT}_n^*(u)\big) = \Delta_n \sum_{i=1}^n e^{-u\hat{c}_i^n}, \quad \text{and}$$

$$C_n^*(u,v) = \Delta_n \sum_{i=1}^n \mathbb{E}^*\big[\xi(u)_i^{n*} - e^{-u\hat{c}_i^n}\big]\big[\xi(v)_i^{n*} - e^{-v\hat{c}_i^n}\big] \tag{11}$$

$$= \Delta_n \sum_{i=1}^n F\Big(\sqrt{u\hat{c}_i^n}, \sqrt{v\hat{c}_i^n}\Big).$$

Throughout the paper, we define the preliminary local spot variance estimator as

$$\hat{c}_{j+(i-1)k_n}^n = \frac{n}{k_n}\sum_{m=1}^{k_n}\big|\Delta_{m+(i-1)k_n}^n X\big|^2 1_{\{|\Delta_{m+(i-1)k_n}^n X| \le u_{n,i}\}}, \tag{12}$$

where $i = 1, \dots, n/k_n$ and $j = 1, \dots, k_n$, with k_n being an arbitrary sequence of integers such that $k_n \to \infty$ and $k_n/n \to 0$, that is, localizing the spot variance estimate in time. Moreover, $u_{n,i}$ is a block-specific threshold sequence defined as $u_{n,i} = \alpha_i \Delta_n^{\varpi}$ for some $\alpha_i > 0$ and $0 < \varpi < 1/2$, which asymptotically eliminates the impact of the (finite variation) jump component.

Proposition 2. *Suppose Assumptions* A *and* B *hold. Moreover, let* $C_n^*(u,v)$ *be defined by* (11) *and the spot variance estimator by* (12). *Then, as* $\Delta_n \to 0$, *it follows that*

$$C_n^*(u,v) \xrightarrow{\mathbb{P}} \int_0^T F(\sqrt{uc_s}, \sqrt{vc_s})\,ds.$$

Remark 2. The proof of Proposition 2, which is provided in the Supplement Appendix S3, follows by applying Jacod and Protter (2012, Theorem 9.4.1); see also the corresponding result in Jacod and Rosenbaum (2013) and the recent extensions in Li and Xiu (2016) and Li, Tauchen, and Todorov (2017) to a more general class of volatility functionals that do not have polynomial growth.

Next, we show that the local Gaussian (LG) bootstrap is first-order valid for the RLT.

Theorem 1. *Assume that* $\xi(u)_i^{n*}$ *are generated as in* (10). *Moreover, suppose Assumptions* A *and* B *hold. Then, for every* $u \in \mathbb{K}$, *where* $\mathbb{K}$ *is a compact subset of* $\mathbb{R}_+$, *and as* $\Delta_n \to 0$, *it follows that*

(a) $\mathcal{S}_n^*(u) \overset{d^*}{\Longrightarrow} \Psi_T(u)$ *on* $l^\infty(\mathbb{K})$ *in probability-*$\mathbb{P}$, *for any compact subset* $\mathbb{K}$ *of* $\mathbb{R}_+$;

(b) $\sup_{x\in\mathbb{R}} |\mathbb{P}^*(\mathcal{S}_n^*(u) \le x) - \mathbb{P}(\mathcal{S}_n(u) \le x)| \overset{\mathbb{P}}{\to} 0$.

Theorem 1 justifies using the LG bootstrap (generated as in (9)) to estimate the distribution of $\mathcal{S}_n(u)$, and thus, to construct bootstrap unstudentized (percentile) intervals for the RLT. These percentile intervals are easy to implement in practice, with the advantage of avoiding explicit reliance on an estimator of the (conditional) asymptotic variance of the RLT. Specifically, for any $u > 0$, we may define a $100(1-\alpha)\%$ symmetric LG-based bootstrap percentile interval for the RLT as

$$\mathcal{IC}_\alpha^*(u) = \big(\mathrm{RLT}_n(u) - \Delta_n^{1/2} p_{1-\alpha}^*(u), \mathrm{RLT}_n(u) + \Delta_n^{1/2} p_{1-\alpha}^*(u)\big), \tag{13}$$

where $p_{1-\alpha}^*(u)$ is the $1-\alpha$ quantile of the bootstrap distribution of $|\mathcal{S}_n^*(u)|$.

Remark 3. The functional pointwise and uniform bootstrap limit theory for the RLT significantly generalizes the pointwise results for realized volatility and beta measures in Hounyo (2019) as well as power-variation-based jump tests in Dovonon et al. (2019), in addition to applying to a nonlinear transformation of the bootstrapped local Gaussian increments. Moreover, relative to Hounyo and Varneskov (2020), who provide a dependent wild bootstrap for empirical CDF statistics at high sampling frequencies, we provide uniform limit theory for functions that are continuous and bounded with respect to the sup-norm, whereas they provide equivalent uniform results for discontinuous functions.

3.3 *Bootstrapping studentized statistics*

Although the bootstrap percentile intervals for the RLT are easy to compute in practice, they may not necessarily be very accurate unless the sample size is large; see, for example, Shao and Tu (1995, Section 4.1.2). In contrast to bootstrap percentile intervals (which rely on asymptotically nonpivotal statistics), we may utilize equivalent bootstrap statistics that are asymptotically pivotal. To this end, this section outlines how the LG bootstrap procedures may be adapted to cover studentized (percentile-t) intervals for the RLT. First, we propose a consistent bootstrap covariance estimator,

$$\widehat{C}_n^*(u,v) = \Delta_n \sum_{i=1}^{n-1} \big(\xi(u)_i^{n*} - e^{-u\hat{c}_i^n}\big)\big(\xi(v)_i^{n*} - e^{-v\hat{c}_i^n}\big),$$

for $u, v > 0$, and form bootstrap studentized (percentile-t) intervals for the RLT as

$$T_n^*(u) = \frac{\Delta_n^{-1/2}\left(\mathrm{RLT}_n^*(u) - \Delta_n \sum_{i=1}^{n} e^{-u\hat{c}_i^n}\right)}{\sqrt{\widehat{C}_n^*(u,u)}}. \tag{14}$$

THEOREM 2. *Suppose the conditions for Theorem 1 hold. Then, for every* $u \in \mathbb{K}$, *where* $\mathbb{K}$ *is a compact subset of* $\mathbb{R}_+$, *and as* $\Delta_n \to 0$, *it follows for* $T_n^*(u)$ *in* (14) *that*

$$\sup_{x\in\mathbb{R}}\left|\mathbb{P}^*\left(T_n^*(u) \le x\right) - \mathbb{P}\left(T_n(u) \le x\right)\right| \xrightarrow{\mathbb{P}} 0.$$

REMARK 4. As for the unstudentized bootstrap confidence intervals in equation (13), the corresponding studentized statistics using the LG bootstrap may be utilized to construct percentile-t intervals for the RLT. To this end, let $\widehat{C}_n(u, v)$ be defined as in (5) and $q^*_{1-\alpha}(u)$ be the $1-\alpha$ quantile of the bootstrap distribution of $|T_n^*(u)|$, constructed as in equation (14). Then, for any $u > 0$, a $100(1-\alpha)\%$ symmetric bootstrap percentile-t confidence interval for RLT may be formed as

$$\begin{aligned}&\mathcal{IC}^*_\alpha(u)\\&\quad= \left(\mathrm{RLT}_n(u) - \Delta_n^{1/2} q^*_{1-\alpha}(u)\sqrt{\widehat{C}_n(u, u)}, \mathrm{RLT}_n(u) + \Delta_n^{1/2} q^*_{1-\alpha}(u)\sqrt{\widehat{C}_n(u, u)}\right).\end{aligned} \tag{15}$$

4. SECOND-ORDER ACCURACY OF THE LG BOOTSTRAP

The higher-order properties of local Gaussian resampling schemes have been thoroughly studied in different contexts; Hounyo (2019) shows that it achieves third-order asymptotic refinements for realized volatility and realized beta inference, and Dovonon et al. (2019) find the scheme to generate second-order improvements in accuracy for jump tests. Motivated, in part, by their results and the excellent finite sample properties of our LG bootstrap, as demonstrated in Section 6 below, we study its higher-order properties in the present setting, where the bootstrap observations have been nonlinearly transformed when computing the RLT and its associated functional limit theory is uniform.

4.1 *A simplified setting for second-order asymptotics*

This section examines whether our LG bootstrap in Section 3.2 can achieve asymptotic refinements through order $O_p(\sqrt{\Delta_n})$ over the standard Gaussian approximation from Theorems 1 and 2 when estimating the distribution function $\mathbb{P}(T_n(u) \le x)$. To this end, we follow the higher-order bootstrap analyses in Gonçalves and Meddahi (2009) and Dovonon et al. (2019) by adopting a simplified model for X, namely

$$X_t = \int_0^t \sigma_s \, dW_s, \tag{16}$$

where σ_t is independent of W_t and $\mathcal{F}_t$-adapted. That is, we not only impose continuous semimartingale dynamics on the process X, we also assume that there is no drift nor leverage effects. Throughout this section, we further let

$$\bar{c}_i^n \equiv \Delta_n^{-1} \int_{(i-1)\Delta_n}^{i\Delta_n} \sigma_t^2 \, dt, \tag{17}$$

and recall that $n = \lfloor T/\Delta_n \rfloor = T/\Delta_n$. In this setting, conditionally on the path of volatility, that is, on $\mathcal{F}$, we have $\Delta_i^n X \sim N(0, \Delta_n \bar{c}_i^n)$, independently across observations $i = 1, \dots, n$. Hence, for cosine transforms $\xi(u)_i^n = \cos(\sqrt{2u}\Delta_n^{-1/2}\Delta_i^n X)$, it follows that $\mathbb{E}[\xi(u)_i^n|\mathcal{F}] = e^{-u\bar{c}_i^n}$.

Despite the more restrictive nature of the setting in (16), a higher-order analysis remains useful for identifying and understanding potential inference improvements from the LG bootstrap. Specifically, we will study the second-order accuracy of the bootstrap by relying on Edgeworth expansions for the distribution of our studentized test statistics $T_n(u)$ and $T_n^*(u)$, which, as is well known from the bootstrap literature (cf., Hall (1992)), is equivalent to studying their first three (conditional) cumulants. For this purpose, let us decompose the studentized RLT-based t-statistic, $T_n(u)$, as

$$T_n(u) = \underbrace{\frac{\Delta_n^{-1/2}\big(\mathrm{RLT}_n(u) - \mathbb{E}\big(\mathrm{RLT}_n(u)|\mathcal{F}\big)\big)}{\sqrt{\widehat{C}_n(u, u)}}}_{\xrightarrow{ds} N(0,1)} + \underbrace{A_n(u)\left(\frac{\widehat{C}_n(u, u)}{C_n(u, u)}\right)^{-1/2}}_{\xrightarrow{\mathbb{P}} 0}, \tag{18}$$

where $\widehat{C}_n(u, u)$ is given by (5), $C_n(u, u) \equiv \mathbb{V}(\Delta_n^{-1/2}\,\mathrm{RLT}_n(u)|\mathcal{F})$, and define

$$\begin{aligned} A_n(u) &\equiv \frac{\Delta_n^{-1/2}\left(\mathbb{E}\big(\mathrm{RLT}_n(u)|\mathcal{F}\big) - \int_0^T e^{-uc_s}\, ds\right)}{\sqrt{C_n(u, u)}} \\ &= \frac{\Delta_n^{-1/2}}{\sqrt{C_n(u, u)}}\left(\Delta_n \sum_{i=1}^n e^{-u\bar{c}_i^n} - \int_0^T e^{-uc_s}\, ds\right). \end{aligned}$$

Furthermore, let $C(u, v) \equiv \operatorname*{plim}_{n\to\infty} C_n(u, v) = \int_0^T F(\sqrt{uc_s}, \sqrt{vc_s})\, ds$. Then, in this simplified setting (16), where X is continuous semimartingale with neither drift nor leverage effects, and with Assumption B holding for the volatility process, the effect of $A_n(u)$ as $\Delta_n \to 0$ is *also* negligible at second order. In particular, Lemma S3 in the Supplementary Appendix formally shows that

$$\Delta_n^{-1/2} A_n(u) \xrightarrow{\mathbb{P}} 0, \tag{19}$$

uniformly in u over a compact subset of $\mathbb{R}_+$, simplifying the analysis of (18).

4.2 *Second-order expansions for the cumulants of* $T_n(u)$ *and* $T_n^*(u)$

First, we provide asymptotic expansions for the cumulants of $T_n(u)$. To this end, let $\kappa_i(T_n(u))$ denote the ith cumulant of $T_n(u)$ for some positive integer i, conditionally on $\mathcal{F}$. Specifically, recall that

$$\begin{aligned} &\kappa_1\big(T_n(u)\big) = \mathbb{E}\big(T_n(u)|\mathcal{F}\big), \qquad \kappa_2\big(T_n(u)\big) = \mathbb{V}\big(T_n(u)|\mathcal{F}\big), \\ &\kappa_3\big(T_n(u)\big) = \mathbb{E}\big(T_n(u) - \mathbb{E}\big(T_n(u)|\mathcal{F}\big)|\mathcal{F}\big)^3. \end{aligned}$$

In addition, define the random variables:

$$\Upsilon_1 \equiv \frac{1}{4\big(C(u,u)\big)^{3/2}} \int_0^T \big(e^{-9uc_s} - 3e^{-uc_s} - 6e^{-5uc_s} + 8e^{-3uc_s}\big)\, ds,$$

$$\Upsilon_2 = \frac{3}{2C(u,u)} \int_0^T \big(e^{-2uc_s} - 1\big)^2 ds, \quad \text{and} \quad (\kappa_1, \kappa_2, \kappa_3) \equiv \big(-\Upsilon_1/2, 1, \Upsilon_1(5 - 3\Upsilon_2)/2\big).$$

THEOREM 3. *Suppose that* (16) *and Assumption* B *hold. Then it follows that*

$$\kappa_1\big(T_n(u)\big) = \sqrt{\Delta_n}\kappa_1 + O_p(\Delta_n), \qquad \kappa_2\big(T_n(u)\big) = 1 + O_p(\Delta_n),$$
$$\kappa_3\big(T_n(u)\big) = \sqrt{\Delta_n}\kappa_3 + O_p(\Delta_n),$$

for every $u \in \mathbb{K}$, *where* $\mathbb{K}$ *is a compact subset of* $\mathbb{R}_+$.

Theorem 3 demonstrates that the first- and third-order cumulants of $T_n(u)$ are subject to a higher-order bias of order $O_p(\sqrt{\Delta_n})$, thus providing the magnitude of the errors for the asymptotic standard Gaussian approximation utilized in the stable limit theory for the RLT. Hence, the LG bootstrap is asymptotically second-order accurate if the corresponding bootstrap cumulants mimic κ_1 and κ_3.

To facilitate a comparison of higher-order errors, write

$$\kappa_1^*\big(T_n^*(u)\big) = \sqrt{\Delta_n}\kappa_{1n}^* + o_p(\sqrt{\Delta_n}) \quad \text{and} \quad \kappa_3^*\big(T_n^*(u)\big) = \sqrt{\Delta_n}\kappa_{3n}^* + o_p(\sqrt{\Delta_n}),$$

where κ_{1n}^* and κ_{3n}^* are the leading terms of the first- and third-order cumulants of $T_n^*(u)$. Importantly, these are functions of the original observations, and thus, depend on the sample size n. Their probability limits, denoted by κ_1^* and κ_3^*, respectively, are derived in the following theorem.

THEOREM 4. *Suppose that* (16) *and Assumption* B *hold. Then it follows that* $\kappa_1^* = \kappa_1$ *and* $\kappa_3^* = \kappa_3$, *where* κ_1 *and* κ_3 *are the limiting cumulant bias terms in Theorem* 3.

Theorem 4 shows that the bootstrap studentized t-statistic $T_n^*(u)$ is able to replicate the first- and third-order cumulants through order $O_p(\sqrt{\Delta_n})$ and, consequently, provides a second-order asymptotic refinement to the (feasible) central limit theory. Interestingly, our second-order result is stronger than the corresponding for jump tests in Dovonon et al. (2019), where a bias-corrected version of the bootstrap studentized t-statistic is needed to obtain refinements through $O_p(\sqrt{\Delta_n})$.

To understand how this bias impacts the first-order cumulant of $T_n(u)$, note that we may write

$$T_n(u) = \big(Z_n(u) + A_n(u)\big)\big(1 + \Delta_n^{1/2}\big(U_n(u) + B_n(u)\big)\big)^{-1/2}, \tag{20}$$

where $Z_n(u) \equiv \Delta_n^{-1/2}(\text{RLT}_n(u) - \mathbb{E}(\text{RLT}_n(u)|\mathcal{F}))/\sqrt{C_n(u,u)}$, and

$$U_n(u) = \frac{\Delta_n^{-1/2}\big(\widehat{C}_n(u,u) - \mathbb{E}\big(\widehat{C}_n(u,u)|\mathcal{F}\big)\big)}{C_n(u,u)},$$

$$B_n(u)=\frac{\Delta_n^{-1/2}\big(\mathbb{E}\big(\widehat{C}_n(u,u)|\mathcal{F}\big)-C_n(u,u)\big)}{C_n(u,u)}.$$

Now, conditionally on σ, we readily have $\mathbb{E}(Z_n(u)|\mathcal{F})=0$ and $\mathbb{V}(Z_n(u)|\mathcal{F})=1$; consequently, the random variable $Z_n(u)$ drives the usual standard Gaussian limiting approximation. On the other hand, the term $A_n(u)$ is known (again, conditionally on σ) and reflects a Jensen's inequality bias for the cosine transformation in the RLT, $\mathbb{E}(\mathrm{RLT}_n(u)|\mathcal{F})-\int_0^T e^{-uc_s}\,ds\neq 0$ for finite n. However, in the proof (cf., Lemma S3), we demonstrate that the probability limit of $\Delta_n^{-1/2}A_n(u)$ is zero and that the bias term $A_n(u)=O_p(\Delta_n)$, implying that to order $O_p(\Delta_n)$, the first-order cumulant of $T_n(u)$ is

$$\kappa_1\big(T_n(u)\big)=\underbrace{\sqrt{\Delta_n}\bigg(\underbrace{\Delta_n^{-1/2}A_n(u)}_{\xrightarrow{\mathbb{P}}0}-\frac{1}{2}\mathbb{E}\big(S_n(u)U_n(u)|\mathcal{F}\big)\bigg)}_{\xrightarrow{\mathbb{P}}\kappa_1}+O_p(\Delta_n).$$

The corresponding bias in Dovonon et al. (2019) is driven by bipower variation (in the jump test) being a biased estimator of integrated variance in finite samples, in particular, having a bias that persists at rate $O_p(\sqrt{\Delta_n})$, implying that it impacts the second-order limit theory. In our setting, this suggests that estimation biases will play a smaller finite sample role for our bootstrap inference.

Importantly, and in contrast to Dovonon et al. (2019) (cf., their Assumption V), the second-order Edgeworth expansions for the cumulants of the t-statistics $T_n(u)$ and $T_n^*(u)$ are derived under the general assumption that the spot volatility obeys a semimartingale process. Specifically, we avoid imposing tight restrictions on the volatility dynamics (like Hölder-continuity of order $\delta>1/2$), thus speaking more directly to the semimartingle setting behind Theorems 1 and 2.

5. Spot Laplace transform and (co)variance inference

Having examined the first- and second-order properties of the LG bootstrap, this section extends its scope by applying it to new high-frequency estimators of spot measures. Specifically, we introduce kernel-weighted Laplace transform-based estimators of the spot variance as well as the spot covariance, beta, and correlation between two semimartingales. Furthermore, we adapt the LG bootstrap to the requisite estimator for drawing inference. The main motivation behind the use of Laplace transforms to design such estimators and inference procedures instead of relying on estimators based on localized power variation (e.g., Jacod and Protter (2012, Chapter 13)) is their (higher-order) robustness toward jumps, which generates improved finite sample performance; see, for example, Jacod and Todorov (2014). However, existing spot variance estimators based on the Laplace transform are very sensitive to the selection of the tuning parameter u, implying a lack of robustness in finite samples. We resolve this issue by integrating across a compact range of u using a prespecified kernel function.

5.1 *Inference for the spot Laplace transform*

We first study inference for the time-varying spot Laplace transform (SLT), defined as $e^{-u\sigma_\tau^2}$ for some local time $\tau \in [0, T]$, which is used by Jacod and Todorov (2014, Section 3), among others, to design efficient integrated variance estimators in the presence of infinite variation jumps. To this end, and for each $i \in \{k_n+1, \dots, n\}$, we define a localized version of the RLT as

$$\mathrm{SLT}_{n,\tau}(u) = \frac{1}{k_n} \sum_{m=1}^{k_n} \xi(u)^n_{i+(m-k_n-1)}, \quad \tau \in ((i-1)\Delta_n, i\Delta_n], \tag{21}$$

setting $\mathrm{SLT}_{n,\tau}(u) = \mathrm{SLT}_{n,(k_n+1)\Delta_n}(u)$ for $0 \le \tau \le k_n + 1$.

THEOREM 5. *Suppose Assumptions A and B hold. Moreover, let the sequence $k_n \to \infty$ as $\Delta_n \to 0$ such that $k_n\sqrt{\Delta_n} \to \vartheta$, for some $0 \le \vartheta < \infty$, it follows that*

$$\mathcal{S}_{n,\tau}(u) \equiv \sqrt{k_n}\big(\mathrm{SLT}_{n,\tau}(u) - e^{-u\sigma_\tau^2}\big) \xrightarrow{d_s} \Phi_\tau(u), \quad \tau \in [0, T],$$

where convergence is on the space $C(\mathbb{R}_+)$ of continuous functions indexed by u and equipped with the local uniform topology (i.e., uniformly over compact sets of $u \in \mathbb{R}_+$). The limiting process $\Phi_\tau(u)$ is an $\mathcal{F}$-conditionally Gaussian process, defined on an extension of the original probability space, and it has zero mean-function and asymptotic variance function on the form,

$$F_\tau(u, v) \equiv F\Big(\sqrt{u\sigma_\tau^2}, \sqrt{v\sigma_\tau^2}\Big) + \frac{\vartheta^2 K_1(\sigma_\tau, u) K_1(\sigma_\tau, v)\big(v_\tau^2 + (v_\tau')^2\big)}{3}, \tag{22}$$

with $F(x, y)$ defined in (4) for $x, y \in \mathbb{R}_+$, and similarly, $K_1(x, u) = -2uxe^{-ux^2}$.

Theorem 5 demonstrates that the functional stable limit theory for the RLT carries over to the localized SLT statistic, with appropriate changes to the asymptotic variance function. Specifically, its two components reflect sampling errors in the formation of the SLT and discretization of the local variance process, respectively. Importantly, by allowing $0 \le \vartheta < \infty$, the SLT can achieve a convergence rate $\Delta_n^{-1/4}$ when setting $k_n \asymp 1/\sqrt{\Delta_n}$, which is known to be optimal in the context of high-frequency spot variance estimation; see, for example, Alvarez, Panloup, Pontier, and Savy (2012), Jacod and Protter (2012, Theorem 13.3.3), and Jacod and Rosenbaum (2015). Furthermore, consistent with the limit theory for a threshold-based spot variance estimator in Jacod and Protter (2012, Theorem 13.3.3), the asymptotic variance simplifies as $F_\tau(u, v) \equiv F(\sqrt{u\sigma_\tau^2}, \sqrt{v\sigma_\tau^2})$ if restricting $k_n\sqrt{\Delta_n} \to 0$, since the volatility discretization errors become asymptotically negligible. Although their focus is on integrated variance estimation, Jacod and Todorov (2014) require $k_n\sqrt{\Delta_n} \to 0$ for their Laplace-based ingredient. Hence, the limit result in Theorem 5 is new to the literature, providing a uniform characterization of the SLT across the two distinct convergence regimes, $\vartheta = 0$ and $0 < \vartheta < \infty$. The suboptimal convergence rate case ($\vartheta = 0$) is included since it becomes useful for developing our bootstrap inference.

The composition of $F_\tau(u,v)$, in particular, its dependence on the term $v_\tau^2+(v_\tau')^2$, renders inference for the SLT statistic highly nontrivial since it is tedious to accurately estimate the local "variance of variance"; see, for example, Jacod and Protter (2012, p. 393), who deem the case $\vartheta=0$ the only practically relevant for inference. Similar comments apply to our LG bootstrap method, at least in its current design, meaning that it is unable to replicate the second term of $F_\tau(u,v)$ in the regime $0<\vartheta<\infty$. Hence, to solve this issue, and provide feasible inference for the SLT, we choose a smaller localization window, $k_n\sqrt{\Delta_n}\to 0$, and adapt our bootstrap procedures for the RLT by defining an equivalent bootstrap SLT estimator as well as an unstudentized test statistic as

$$\begin{aligned}\mathrm{SLT}^*_{n,\tau}(u)&\equiv\frac{1}{k_n}\sum_{m=1}^{k_n}\xi(u)^{n*}_{i+(m-k_n-1)},\\ \mathcal{S}^*_{n,\tau}(u)&\equiv\sqrt{k_n}\big(\mathrm{SLT}^*_{n,\tau}(u)-\mathbb{E}^*\big(\mathrm{SLT}^*_{n,\tau}(u)\big)\big).\end{aligned}\tag{23}$$

THEOREM 6. *Let $\mathcal{S}^*_{n,\tau}(u)$ denote the bootstrap statistic (23), where the sequence $(\xi(u)^{n*}_i)_{i=1}^n$ is generated using the LG resampling in (10). Moreover, let the sequence $k_n\to\infty$ as $\Delta_n\to 0$ such that $k_n\sqrt{\Delta_n}\to 0$, then for every $u\in\mathbb{K}$, where $\mathbb{K}$ is a compact subset of $\mathbb{R}_+$, it follows that*

(a) $\mathcal{S}^*_{n,\tau}(u)\xrightarrow{d^*}\Phi_\tau(u)$ *on $l^\infty(\mathbb{K})$ in probability-$\mathbb{P}$, for any compact subset $\mathbb{K}$ of $\mathbb{R}_+$.*

(b) $\sup_{x\in\mathbb{R}}|\mathbb{P}^*(\mathcal{S}^*_{n,\tau}(u)\le x)-\mathbb{P}(\mathcal{S}_{n,\tau}(u)\le x)|\xrightarrow{\mathbb{P}}0.$

Theorem 6 shows that our bootstrap inference procedures extend to spot Laplace transforms by formally establishing their first-order asymptotic validity. While the SLT estimator can achieve the optimal rate of convergence, our bootstrap inference can get arbitrarily close to $\Delta_n^{-1/4}$, but is likely to perform better when the second term in $F_\tau(u,v)$ is small relative to the first term.

5.2 *Spot volatility estimation and inference*

The uniform properties of the SLT (in u) and its associated bootstrap(s) are utilized in designing a new class of spot variance estimators and inference procedures. Specifically, we introduce the class

$$\mathcal{V}_{n,\tau}\equiv-\int_{u_{\min}}^{u_{\max}}\frac{\log\Big(\mathrm{SLT}_{n,\tau}(u)\vee\frac{1}{\sqrt{k_n}}\Big)}{u}\times\mathcal{W}(du),\tag{24}$$

where $\mathcal{W}(du)=W(u)\,du$ is a weight measure with the property $\int_{u_{\min}}^{u_{\max}}\mathcal{W}(du)=1$. These estimators are related to the spot variance "ingredient" in Jacod and Todorov (2014). Specifically, they apply a similar nonlinear transformation of the SLT, which, however, is evaluated at a single u rather than integrated over a range, $u\in[u_{\min},u_{\max}]$. Our design is motivated by the GMM inference procedure for stochastic volatility models in Todorov, Tauchen, and Grynkiv (2011), who integrate the realized Laplace transform over a range to harness most of its information. In particular, we leverage a similar idea in the context of the SLT to achieve robust estimation of the spot variance. Naturally, the estimators (24) nest the corresponding in Jacod and Todorov (2014) for Dirac weights at a point $u \in [u_{\min}, u_{\max}]$. However, it also includes alternative weight functions such as Gaussian and uniform kernels, thus bearing resemblance to the kernel-weighted empirical characteristic function-based estimation procedures in Jiang and Knight (2002) and Carrasco, Chernov, Florens, and Ghysels (2007) for continuous time processes. Interestingly, the simulation study below, indeed, demonstrates that the use of more general weight functions results in substantially less sensitive estimates of spot measures than when relying on a single u.

First, we leverage the uniform limit theory for the SLT (again, as a function of u) to establish corresponding central limit theory for the class of spot variance estimators (24).

Theorem 7. *Suppose the conditions of Theorem 5 hold. Then it follows that*

$$\mathcal{SV}_{n,\tau} \equiv \sqrt{k_n}\big(\mathcal{V}_{n,\tau} - \sigma_\tau^2\big) \xrightarrow{d_s} \Upsilon_\tau, \tag{25}$$

where Υ_τ is an $\mathcal{F}$-conditionally Gaussian random variable, defined on an extension of the original probability space, which has a zero mean and, with $F_\tau(u,v)$ defined as in (22), asymptotic variance,

$$\Xi_\tau = \int_{u_{\min}}^{u_{\max}} \int_{u_{\min}}^{u_{\max}} \frac{F_\tau(u,v)W(u)W(v)}{uve^{-(u+v)\sigma_\tau^2}}\,du\,dv.$$

The new class of spot variance estimators (24) inherits the properties of the SLT, implying that they can achieve the optimal rate of convergence, $\Delta_n^{-1/4}$. Moreover, to draw inference on the spot variance, we define the bootstrap analogs of $\mathcal{V}_{n,\tau}$ and $\mathcal{SV}_{n,\tau}$ as

$$\begin{aligned}
\mathcal{V}^*_{n,\tau} &\equiv -\int_{u_{\min}}^{u_{\max}} \frac{\log\left(\mathrm{SLT}^*_{n,\tau}(u) \vee \frac{1}{\sqrt{k_n}}\right)}{u} \times \mathcal{W}(du), \quad \text{and} \\
\mathcal{SV}^*_{n,\tau} &\equiv \sqrt{k_n}\left(\mathcal{V}^*_{n,\tau} + \int_{u_{\min}}^{u_{\max}} \frac{\log\left(\mathbb{E}^*\big(\mathrm{SLT}^*_{n,\tau}(u)\big) \vee \frac{1}{\sqrt{k_n}}\right)}{u} \times \mathcal{W}(du)\right),
\end{aligned} \tag{26}$$

respectively, thus mimicking the transformation of the spot variance estimator.

Theorem 8. *Suppose the conditions of Theorem 6 hold. Then it follows that*

$$\sup_{x\in\mathbb{R}} \left|\mathbb{P}^*\big(\mathcal{SV}^*_{n,\tau} \le x\big) - \mathbb{P}(\mathcal{SV}_{n,\tau} \le x)\right| \xrightarrow{\mathbb{P}} 0.$$

Remark 5. As in Jacod and Protter (2012, Chapter 13), who advocate selecting $k_n\sqrt{\Delta_n} \to 0$ as the only empirically interesting case for spot variance estimators because their asymptotic variance can be estimated, our bootstrap procedures facilitate near-efficient inference. However, when only the point estimates are of interest, and not their confidence intervals, our class of spot variance estimators can achieve the optimal rate of convergence, $\Delta_n^{-1/4}$. The same comments apply to all subsequent estimators of multivariate spot measures. Furthermore, our LG bootstrap resampling scheme can be adapted to other spot variance estimators in the literature, for example, the threshold local realized variance estimator studied by Jacod and Protter (2012, Theorem 13.3.3), under similar assumptions on k_n.

REMARK 6. It is instructive to compare the asymptotic variance of our spot variance estimator (24) to the asymptotically efficient threshold local realized volatility (TLRV) estimator, defined via (12), for $\tau \in ((i-1)\Delta_n, i\Delta_n]$ as

$$\mathrm{TLRV}_{n,\tau} = \frac{n}{k_n} \sum_{m=1}^{k_n} \left|\Delta_{i+(m-k_n-1)}^n X\right|^2 1_{\{|\Delta_{i+(m-k_n-1)}^n X| \le u_{n,i}\}}, \tag{27}$$

where, again, $u_{n,i} = \alpha_i \Delta_n^{\varpi}$ for some $\alpha_i > 0$ and $0 < \varpi < 1/2$. The main advantage of the SLT-based estimator is its higher-order robustness toward jumps (Jacod and Todorov, 2014). To examine the trade-off in terms of efficiency, recall the asymptotic variance for TLRV is $2\sigma_\tau^4$, implying that the asymptotic relative efficiency (ARE) of our estimator to the TLRV may be expressed as

$$\begin{aligned}\mathrm{ARE}(\mathcal{V}_{n,\tau}, \mathrm{TLRV}_{n,\tau}) &= \frac{\Xi_\tau}{2\sigma_\tau^4} \\ &= \int_{u_{\min}}^{u_{\max}} \int_{u_{\min}}^{u_{\max}} \frac{\left(e^{\sqrt{uv}\sigma_\tau^2} - e^{-\sqrt{uv}\sigma_\tau^2}\right)^2}{4uv\sigma_\tau^4} W(u)W(v)\,du\,dv,\end{aligned} \tag{28}$$

where, for simplicity, we have let $k_n\sqrt{\Delta_n} \to 0$ such that $F_\tau(u,v) = F(\sqrt{u\sigma_\tau^2}, \sqrt{v\sigma_\tau^2})$. The double integral is hard to evaluate. Hence, we study an approximation and visualize the ARE for fixed choices of $u_{\min}$, $u_{\max}$ and σ_τ. Specifically, when $\sqrt{uv}\sigma_\tau^2$ is small, a Maclaurin expansion delivers

$$\begin{aligned}\mathrm{ARE}(\mathcal{V}_{n,\tau}, \mathrm{TLRV}_{n,\tau}) &\simeq \int_{u_{\min}}^{u_{\max}} \int_{u_{\min}}^{u_{\max}} O\left(\frac{\left(\sqrt{uv}\sigma_\tau^2\right)^2}{6}\right) W(u)W(v)\,du\,dv \\ &\le 1 + O\left(\left(u_{\max}\sigma_\tau^2\right)^2/6\right).\end{aligned}$$

That is, the loss of relative estimation efficiency is approximately of order $O((u_{\max}\sigma_\tau^2)^2/6)$, which is small if either the tuning parameter $u_{\max}$ or the spot variance, σ_τ, is close to zero. We implement two simple experiments to visualize this feature. First, we let $u_{\min} = 0.01$, $u_{\max} = 1$ and consider $\sigma_\tau \in [0.01, 1]$. Second, we fix $u_{\min} = 0.01$, $\sigma_\tau = 0.5$ and examine $u_{\max} \in [0.01, 2]$. Figure 1 displays these experiments for uniform and exponential weight functions, $W(\cdot)$.

The results in Figure 1 are striking, showing that $\mathcal{V}_{n,\tau}$ exhibits no significant loss of asymptotic efficiency relative to $\mathrm{TLRV}_{n,\tau}$ as long as the spot volatility is less than 50% or if we select $u_{\max} \le 1/2$. Importantly, within these ranges, the choice between equal and

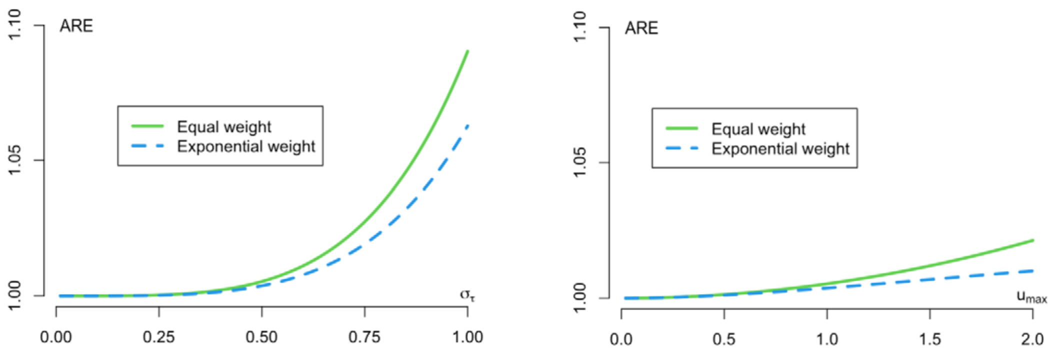

FIGURE 1. Asymptotic relative efficiency. In the left panel, ARE is depicted with $u_{\min} = 0.01$ and $u_{\max} = 1$ fixed. In the right panel, ARE is depicted with $u_{\min} = 0.01$ and $\sigma = 0.5$ fixed.

exponential weight functions is also immaterial. Fortunately, in most financial applications, the spot volatility will be substantially smaller than 50%, suggesting there is essentially no efficiency loss from using $\mathcal{V}_{n,\tau}$ instead of $\mathrm{TLRV}_{n,\tau}$. Finally, from the right-hand side panel, our results suggest to choose $u_{\max} \leq 1/2$ to avoid efficiency losses, which will guide our tuning parameters selections in the simulation study below.

REMARK 7. Since the estimators (24) involve a nonlinear transformation of the SLT, we have considered a class of second-order bias-corrected estimators, via a Taylor expansion. However, unreported simulations document only small numerical differences between this and (24).

REMARK 8. We conjecture that results similar to Theorems 7 and 8 will continue to hold when the semimartingale process X_t in equation (1) contains a jump component that is of infinite variation, using the techniques and asymptotic analyses in Jacod and Todorov (2014), Liu, Liu, and Liu (2018), and Liu and Liu (2020) for the (nonbootstrap, non-u-kernel weighted) inference on spot variance, covariance, and beta. A formal treatment of infinite variation jumps is beyond the scope of the paper.

5.3 *Spot covariance, correlation, and beta inference*

We further broaden the scope of our bootstrap procedures by adapting them to draw inference on statistics, which are constructed as smooth transformations of the spot covariance between two semimartingales. To this end, we first introduce a new Laplace-based estimator of the spot covariance that utilizes the polarization identity. Moreover, we extend the univariate dynamic setting in (1) by stipulating that the two processes X and Y obey the bivariate system of differential equations,

$$dX_t = a_{1t}\,dt + \sigma_{1t}\,dW_{1t} + \int_{\mathbb{R}} \delta_1(t-, x)\mu_1(dt, dx), \tag{29}$$

$$dY_t = a_{2t}\,dt + \sigma_{2t}\Big(\rho_t\,dW_{1t} + \sqrt{1-\rho_t^2}\,dW_{2t}\Big) + \int_{\mathbb{R}} \delta_2(t-, x)\mu_2(dt, dx), \tag{30}$$

where the drifts α_j, volatilities σ_j, and the correlation ρ are $(\mathcal{F}_t)$-adapted processes with càdlàg paths for $j = 1, 2$, $\boldsymbol{W} = (W_1, W_2)'$ is a 2-dimensional standard Brownian motion, μ_j (again, $j = 1, 2$) is a homogeneous Poisson measure with compensator $dt \otimes \nu_j(dx)$, ν_j is a Lévy measure and $\delta_j(t, x) : \mathbb{R}_+ \times \mathbb{R} \to \mathbb{R}$ are càdlàg in t. This bivariate system represents a natural extension of (1) and we require formal (yet, mild) regularity conditions on the components of the model that mimic those in Assumptions A and B. Hence, they are deferred to Appendix A for ease of exposition.

We are interested in drawing inference on the following spot measures:

$$\begin{aligned} C_\tau(X, Y) &= \rho_\tau \sigma_{1\tau} \sigma_{2\tau}, \\ \rho_\tau(X, Y) &= \frac{C_\tau(X, Y)}{\sqrt{C_\tau(X, X) C_\tau(Y, Y)}}, \\ \beta_\tau(X, Y) &= \frac{C_\tau(X, Y)}{C_\tau(X, X)}, \end{aligned} \tag{31}$$

for some $\tau \in [0, T]$, thus capturing the spot covariance, correlation, and beta, respectively. Hence, let us write $\mathrm{SLT}_{n,\tau}(u, Z)$ and $\mathcal{V}_{n,\tau}(Z)$ to emphasize that the SLT and spot variance estimators in equations (21) and (24), respectively, are computed using variable Z. We, then, use the polarization identity to introduce a jump-robust Laplace-based estimator of the spot covariance between X and Y,

$$C_{n,\tau}(X, Y) = \frac{1}{4}\big(\mathcal{V}_{n,\tau}(X + Y) - \mathcal{V}_{n,\tau}(X - Y)\big), \tag{32}$$

as well as to design corresponding jump-robust estimators of spot correlation and spot beta,

$$\rho_{n,\tau}(X, Y) = \frac{C_{n,\tau}(X, Y)}{\sqrt{C_{n,\tau}(X, X) C_{n,\tau}(Y, Y)}} \quad \text{and} \quad \beta_{n,\tau}(X, Y) = \frac{C_{n,\tau}(X, Y)}{C_{n,\tau}(X, X)}, \tag{33}$$

respectively, whose asymptotic properties are provided by the following theorem.

Theorem 9. *Suppose the conditions of Theorem 5 and Assumption B′ hold. Then it follows that*

(a) $\mathcal{SV}_{n,C_\tau} \equiv \sqrt{k_n}(C_{n,\tau}(X, Y) - C_\tau(X, Y)) \xrightarrow{d_s} \Gamma_{C_\tau}$.

(b) $\mathcal{SV}_{n,\rho_\tau} \equiv \sqrt{k_n}(\rho_{n,\tau}(X, Y) - \rho_\tau(X, Y)) \xrightarrow{d_s} \Gamma_{\rho_\tau}$.

(c) $\mathcal{SV}_{n,\beta_\tau} \equiv \sqrt{k_n}(\beta_{n,\tau}(X, Y) - \beta_\tau(X, Y)) \xrightarrow{d_s} \Gamma_{\beta_\tau}$,

where Γ_{C_τ}, Γ_{ρ_τ} and Γ_{β_τ} are $\mathcal{F}$-conditionally Gaussian random variables, defined on an extension of the original probability space, have zero means and have variances that are given in the Online Appendix.

The analytical expressions for the asymptotic variances of Γ_{C_τ}, Γ_{ρ_τ}, and Γ_{β_τ} are cumbersome, even when selecting $k_n\sqrt{\Delta_n} \to 0$. This makes our proposed bootstrap procedures particularly attractive for drawing inference on the spot measures in (31) since the construction of confidence intervals using unstudentized (percentile) methods circumvent explicit estimation of the asymptotic variances. We need to modify the LG bootstrap to capture cross-dependence between X and Y in the resampling. Specifically, inspired by Hounyo (2019, equation (18)), we generate bivariate increments as

$$\begin{pmatrix} \Delta_i^n X^* \\ \Delta_i^n Y^* \end{pmatrix} = \sqrt{\Delta_n} \begin{pmatrix} \sqrt{\hat{c}_i^n(X, X)} & 0 \\ \dfrac{\hat{c}_i^n(X, Y)}{\sqrt{\hat{c}_i^n(X, X)}} & \sqrt{\hat{c}_i^n(Y, Y) - \dfrac{\hat{c}_i^n(X, Y)^2}{\hat{c}_i^n(X, X)}} \end{pmatrix} \begin{pmatrix} \eta_{1i}^* \\ \eta_{2i}^* \end{pmatrix}, \tag{34}$$

$i = 1, \dots, n$, where $(\eta_{1i}^*, \eta_{2i}^*)' \sim$ i.i.d. $N(0, I_2)$, with I_2 being a two-dimensional identity matrix, and

$$\begin{aligned} &\begin{pmatrix} \hat{c}_i^n(X, X) & \hat{c}_i^n(Y, X) \\ \hat{c}_i^n(X, Y) & \hat{c}_i^n(Y, Y) \end{pmatrix} \\ &\quad \equiv \frac{n}{k_n} \sum_{m=1}^{jk_n} \begin{pmatrix} \Delta_{m+(i-1)k_n}^n X \\ \Delta_{m+(i-1)k_n}^n Y \end{pmatrix} \begin{pmatrix} \Delta_{m+(i-1)k_n}^n X \\ \Delta_{m+(i-1)k_n}^n Y \end{pmatrix}' \mathbf{1}_n(X, Y), \end{aligned} \tag{35}$$

for $i = 1, \dots, \lfloor n/k_n \rfloor$ and $j = 1, \dots, k_n$, where we have defined

$$\mathbf{1}_n(X, Y) \equiv 1\{|\Delta_{m+(i-1)k_n}^n X| \leq u_{n,i}(X), |\Delta_{m+(i-1)k_n}^n Y| \leq u_{n,i}(Y)\},$$

for local jump-truncation sequences $u_{n,i}(X)$ and $u_{n,i}(Y)$ satisfying the properties in (12).

We apply this modified LG resampling scheme to construct Laplace transform-based bootstrap estimators of the spot covariance, correlation, and beta, respectively, as

$$\begin{aligned} C_{n,\tau}^*(X, Y) &= \frac{1}{4}\big(\mathcal{V}_{n,\tau}^*(X + Y) - \mathcal{V}_{n,\tau}^*(X - Y)\big), \\ \rho_{n,\tau}^*(X, Y) &= \frac{C_{n,\tau}^*(X, Y)}{\sqrt{C_{n,\tau}^*(X, X) C_{n,\tau}^*(Y, Y)}}, \quad \text{and} \\ \beta_{n,\tau}^*(X, Y) &= \frac{C_{n,\tau}^*(X, Y)}{C_{n,\tau}^*(X, X)}, \end{aligned}$$

with $\mathrm{SLT}_{n,\tau}^*(u, Z)$ and $\mathcal{V}_{n,\tau}^*(Z)$, similarly, being the bootstrap SLT and spot variance estimator, respectively, using variable Z^*. Moreover, we define the corresponding bootstrap (unstudentized) test statistics as $\mathcal{SV}_{n,C_\tau}^* \equiv \sqrt{k_n}(C_{n,\tau}^*(X, Y) - \mathbb{E}_{C_\tau^n(X,Y)}^*)$ for spot covariance, along with

$$\begin{aligned} \mathcal{SV}_{n,\rho_\tau}^* &\equiv \sqrt{k_n}\left(\rho_{n,\tau}^*(X, Y) - \frac{\mathbb{E}_{C_\tau^n(X,Y)}^*}{\sqrt{\mathbb{E}_{C_\tau^n(X,X)}^* \mathbb{E}_{C_\tau^n(Y,Y)}^*}}\right), \\ \mathcal{SV}_{n,\beta_\tau}^* &\equiv \sqrt{k_n}\left(\beta_{n,\tau}^*(X, Y) - \frac{\mathbb{E}_{C_\tau^n(X,Y)}^*}{\mathbb{E}_{C_\tau^n(X,X)}^*}\right), \end{aligned}$$

for spot correlation and beta, respectively, where

$$\mathbb{E}^*_{C^n_\tau(X,Y)} \equiv -\int_{u_{\min}}^{u_{\max}} \frac{\log\left(\mathbb{E}^*\left(\mathrm{SLT}^*_{n,\tau}(u, X+Y)\right) \vee \frac{1}{\sqrt{k_n}}\right)}{4u} \times \mathcal{W}(du)$$
$$+\int_{u_{\min}}^{u_{\max}} \frac{\log\left(\mathbb{E}^*\left(\mathrm{SLT}^*_{n,\tau}(u, X-Y)\right) \vee \frac{1}{\sqrt{k_n}}\right)}{4u} \times \mathcal{W}(du),$$

and $\mathbb{E}^*_{C^n_\tau(Z,Z)}$ is defined analogously for $Z = (X, Y)'$. We are now ready to establish first-order asymptotic validity of our bootstrap inference procedures for the spot measures (31).

Theorem 10. *Suppose the conditions of Theorem 6 and Assumption B′ hold. Moreover, let the LG bootstrap follow the modified resampling scheme in* (34) *and* (35). *Then it follows that*

(a) $\sup_{x\in\mathbb{R}} |\mathbb{P}^*(\mathcal{SV}^*_{n,C_\tau} \le x) - \mathbb{P}(\mathcal{SV}_{n,C_\tau} \le x)| \xrightarrow{\mathbb{P}} 0$.

(b) $\sup_{x\in\mathbb{R}} |\mathbb{P}^*(\mathcal{SV}^*_{n,\rho_\tau} \le x) - \mathbb{P}(\mathcal{SV}_{n,\rho_\tau} \le x)| \xrightarrow{\mathbb{P}} 0$.

(c) $\sup_{x\in\mathbb{R}} |\mathbb{P}^*(\mathcal{SV}^*_{n,\beta_\tau} \le x) - \mathbb{P}(\mathcal{SV}_{n,\beta_\tau} \le x)| \xrightarrow{\mathbb{P}} 0$.

This result shows that our bootstrap procedures may not only be used to draw fixed-span inference on the RLT statistic; they can be adapted to (multivariate) spot measures that are critical for risk management and portfolio selection in financial economics, among others.

6. Simulation study

In this section, we assess the finite sample properties of our LG bootstrap for the RLT, drawing comparisons to the feasible limit theory in Section 2 and wild bootstrap alternatives. Moreover, we examine the accuracy of our jump-robust Laplace transform-based spot variance, covariance, correlation, and beta estimators as well as their associated bootstrap inference, provided in Section 5.

6.1 *Confidence intervals for the RLT*

The LG bootstrap procedure yield coverage of the RLT, which is first-order valid and even offer second-order asymptotic refinements. Nonetheless, we expand on the theoretical results by studying its finite sample properties via simulations. To this end, the latent process $\{X_t, t \ge 0\}$ is assumed to be observed in the time interval $[0, 1]$ at a discrete and equidistant time grid $\{i/n, i = 1, 2, \dots, n\}$, with initial value $X_0 = 0$. Specifically, we consider three data generating processes (DGPs). The first two are inspired by Monte Carlo designs from the high-frequency financial econometrics literature; namely, those in Gonçalves and Meddahi (2009) and Wang, Liu, and Xia (2019). The last DGP is adapted from a recent macro-finance model with stochastic volatility. This allows us to assess how our LG resampling procedure performs in different and empirically relevant settings.

Model 1. A one-factor stochastic volatility model with jumps:

$$dX_t = 0.03\,dt + \sigma_t\,dW_t + \sum_{i=1}^{N_t} Y_i, \qquad \sigma_t = \exp(0.3125 - 0.125\tau_t),$$

where $d\tau_t = -0.025\tau_t\,dt + dB_t$ and (B_t, W_t) are two mutually independent Brownian motions, N_t is a Poisson process with intensity $\lambda = 4$, and jump sizes $Y_i \sim$ i.i.d. $N(0, 0.01)$.

Model 2. A two-factor stochastic volatility model with jumps:

$$dX_t = 0.0314\,dt + \sigma_t\Big[\rho_1\,dW_{1t} + \rho_2\,dW_{2t} + \sqrt{1-\rho_1^2-\rho_2^2}\,dW_{3t}\Big] + \sum_{i=1}^{N_t} Y_i,$$

where (W_1, W_2, W_3) are three independent Brownian processes, $\rho_1 = \rho_2 = -0.3$, and the stochastic volatility process decomposes $\sigma_t = \exp(-1.2 + 0.04\sigma_{1t}^2 + 1.5\sigma_{2t}^2)$, with

$$\begin{aligned} d\sigma_{1t}^2 &= -0.00137\sigma_{1t}^2\,dt + dW_{1t}, \\ d\sigma_{2t}^2 &= -1.386\sigma_{2t}^2\,dt + \big(1 + 0.25\sigma_{2t}^2\big)\,dW_{2t}. \end{aligned}$$

Finally, N_t is a Poisson process with intensity $\lambda = 4$, and jump sizes $Y_i \sim$ i.i.d. $N(0, 0.01)$.

Model 3. A macro-finance model with stochastic volatility.[1] Specifically, we adapt the multivariate asset pricing system from Campbell, Giglio, Polk, and Turley (2018) to the present setting, that is, we consider

$$\Delta\boldsymbol{X}_t = (\boldsymbol{\mu} + \boldsymbol{A}\boldsymbol{X}_{t-1})\Delta_n + \sigma_{t-1}\boldsymbol{U}_t,$$

where $\boldsymbol{X}_t$ is a 6-dimensional vector, having asset returns as the first element, σ_t as the second and the last four elements are made up of persistent state variables (price-earnings ratio, 3-month T-bill yield, small-stock value spread, and the default spread). Moreover, $\boldsymbol{\mu}$ is a 6-dimensional constant vector, $\boldsymbol{A}$ is a 6×6 square parameter matrix, $U_t \sim$ i.i.d. $N(\mathbf{0}, \Delta_n\boldsymbol{\Sigma})$. We adopt the parameter values from Campbell et al. (2018, Table 1). These are given in Appendix B for completeness.

We consider the LG bootstrap and four alternative inference procedures for the RLT: one based on the feasible central limit theory (CLT) in Section 2.2; one based on the

[1] Besides giving the simulation study a broader appeal, this macro-finance model is motivated by the results in, for example, Sims and Zha (1999), who showed that Edgeworth expansions may not be very accurate for multivariate models when some series are very persistent, yet still stationary. Hence, we examine the properties of our LG bootstrap for a multivariate asset pricing system with stochastic volatility, where some of the state variables are indeed persistent.

modified wild (MW) bootstrap procedure from our companion note, Hounyo, Liu, and Varneskov (2022); one based on the adaptation of the Wu (1986) and Liu (1988) to the present setting; and, finally, one based on the wild bootstrap from Gonçalves and Meddahi (2009). The last two, dubbed the WL and GM bootstrap procedures, respectively, are discussed in Appendix C.[2] To implement the LG bootstrap, we apply (9) and (12), where the latter is designed with the jump-truncation sequence $u_{n,i} = 7\sqrt{BV_{n,i}}\Delta_n^{0.4}$, with

$$BV_{n,i} = \frac{n\pi}{2k_n} \sum_{m=1}^{k_n-1} \left|\Delta^n_{m+(i-1)k_n} X\right| \left|\Delta^n_{m+1+(i-1)k_n} X\right|$$

being a preliminary local bipower variation estimate of the spot variance process. This tuning parameter selection is motivated by the corresponding choices in Podolskij and Ziggel (2010), Jacod and Todorov (2014), and Dovonon et al. (2019). The MW, GM, and WL bootstrap procedures are implemented with external random variables of the form $\eta_i^* \sim$ i.i.d. $N(0, 1/\sqrt{2})$, which satisfies the conditions of Hounyo, Liu, and Varneskov (2022, Theorem 1).[3] Consequently, the three alternative methods differ only with respect to their (lack of) centering for the bootstrap pseudo observations, $(\xi(u)_i^{n*})_{i=1}^n$.

We consider four different sample sizes: $1/\Delta_n = \{12, 48, 78, 288\}$, corresponding to 2-hour, half-hour, 18.5-minute, and 5-minute returns for observations on financial assets that are traded round-the-clock, such as currencies and various futures contracts. Moreover, we apply block sizes $k_n = \{4, 6, 13, 18\}$ for $n = \{12, 48, 78, 288\}$, respectively, when constructing preliminary spot variance estimates. Bootstrap confidence intervals are generated using 999 draws, and we consider both studentized and unstudentized intervals for all methods. Finally, we implement the RLT and its associated fixed-span inference procedures for Laplace tuning parameters $u = \{1/20, 1/10, 1/5\}$, in line with the magnitudes considered by Jacod and Todorov (2014) and Todorov (2015) in different contexts.

Table 1 provides the actual 95% coverage rates for all confidence intervals across 10,000 replications. There are several interesting observations. First, the intervals based on feasible CLT undercover for all DGPs, especially for small sample sizes n. Second, the MW bootstrap performs similar to the feasible CLT, and so does the studentized intervals for the GM and WL bootstrap procedures. Third, the unstudentized intervals for GM overcovers, always containing the (true) Laplace transform of volatility, while the WL bootstrap dramatically undercovers. These results clearly illustrate the failure of both wild bootstrap procedures to replicate the mean heterogeneity for the sequence of cosine transforms, $(\xi(u)_i^n)_{i=1}^n$. Fourth, the LG bootstrap provides excellent coverage, uniformly improving upon the CLT for all sample sizes. Although derived in a simpler set-

[2] Whereas the WL and GM bootstrap procedures deliver inconsistent inference, the MW bootstrap is first-order asymptotically valid. The main difference arises from the centering of the resampling; see Hounyo, Liu, and Varneskov (2022) for details.

[3] We have also examined the wild bootstrap procedures with external random variables based on the Rademacher distribution and a different two-point distribution. However, since the results for these resampling schemes are very similar to those obtained from the normal distribution, they have been omitted for ease of exposition.

Table 1. RLT coverage.

Nominal 95% coverage rates for the RLT											
				MW		GM		WL		LG	
Model	$u =$	$n =$	CLT	Perc	Perc-t	Perc	Perc-t	Perc	Perc-t	Perc	Perc-t
1	1/20	12	84.09	84.69	80.72	100	84.05	73.99	84.14	88.79	90.27
1	1/20	48	91.98	92.48	91.64	100	91.98	81.00	91.93	94.03	95.39
1	1/20	78	93.45	93.55	92.91	100	93.42	82.26	93.42	94.16	95.22
1	1/20	288	95.18	94.10	93.80	100	95.17	82.77	95.11	94.53	94.91
1	1/10	12	85.70	85.11	81.41	99.88	85.47	75.86	85.57	89.24	89.84
1	1/10	48	92.13	92.56	91.62	100	92.27	80.93	92.19	93.78	94.43
1	1/10	78	93.72	93.84	93.23	99.98	93.66	82.14	93.63	94.12	95.02
1	1/10	288	94.35	94.81	94.66	99.99	94.40	82.70	94.38	94.85	95.42
1	1/5	12	86.18	86.02	82.56	98.11	86.32	76.28	86.26	89.45	89.44
1	1/5	48	93.24	92.99	92.21	98.79	93.22	82.43	93.16	93.35	93.83
1	1/5	78	93.81	93.81	93.37	98.96	94.09	82.99	94.19	93.92	94.14
1	1/5	288	94.60	94.62	94.55	99.16	94.77	83.14	94.81	94.52	94.67
2	1/20	12	77.14	77.15	72.75	100	77.06	70.91	77.20	82.12	81.04
2	1/20	48	87.34	87.45	85.78	100	86.70	80.18	86.82	90.86	91.37
2	1/20	78	89.64	89.61	88.66	100	90.35	84.08	90.38	92.53	92.52
2	1/20	288	93.19	93.25	92.72	99.99	93.57	86.78	93.58	94.15	94.72
2	1/10	12	76.97	76.91	72.66	99.99	78.35	72.03	78.43	82.16	81.98
2	1/10	48	88.02	88.03	86.47	99.99	88.23	81.91	88.16	90.91	91.46
2	1/10	78	89.99	89.89	88.94	99.98	90.27	83.40	90.21	92.42	92.77
2	1/10	288	93.62	93.54	93.18	100	93.38	86.33	93.59	94.54	94.75
2	1/5	12	77.98	77.82	73.51	99.95	78.07	72.01	77.98	82.94	81.91
2	1/5	48	88.81	88.72	87.15	99.95	88.32	81.83	88.32	91.67	92.31
2	1/5	78	89.74	89.67	88.63	100	89.45	82.97	89.53	92.46	93.41
2	1/5	288	94.10	94.07	93.70	99.97	93.20	86.64	93.20	94.67	95.07
3	1/20	12	79.68	79.30	73.10	100	79.70	66.22	79.53	82.32	81.11
3	1/20	48	88.61	87.86	86.23	100	88.71	75.10	88.56	91.04	91.36
3	1/20	78	90.57	89.32	88.25	100	90.40	77.26	90.60	92.32	92.41
3	1/20	288	93.35	93.06	92.64	100	93.43	81.87	93.49	94.44	94.62
3	1/10	12	79.75	78.97	73.88	100	79.72	67.30	79.78	82.67	81.76
3	1/10	48	88.28	88.03	86.42	100	88.13	74.54	88.27	90.78	91.88
3	1/10	78	90.27	90.13	88.99	100	90.22	76.96	90.26	93.12	93.29
3	1/10	288	93.12	93.36	93.12	100	93.06	81.38	93.08	94.77	94.43
3	1/5	12	79.92	79.22	73.24	100	80.07	67.34	79.87	83.66	81.68
3	1/5	48	88.30	88.73	87.24	100	88.24	75.17	88.31	90.88	92.35
3	1/5	78	90.02	90.29	89.19	100	89.93	77.50	89.92	93.01	93.65
3	1/5	288	92.91	93.68	93.35	100	92.99	81.17	92.87	94.48	94.74

Note: This table displays empirical coverage rates for the RLT using different inference procedures. Specifically, these are actual 95% coverage intervals based on the feasible CLT in (6); LG denotes the local Gaussian bootstrap; MW, GM, and WL are different wild bootstrap procedures based on external variables, η_i, that are drawn from a Gaussian distribution. The simulations are implemented with 10,000 replications, each of which uses 999 bootstrap draws. Models 1 and 2 indicate stochastic volatility models with one, respectively, two volatility factors. Model 3 is a macro-finance model inspired by empirical estimates in Campbell et al. (2018).

ting without drift, leverage effects, and jumps, this illustrates the second-order asymptotic refinement result in Theorem 4. Moreover, all procedures have lower coverage for Models 2 and 3 than for Model 1, especially in smaller samples, speaking directly to the finite sample impact of the Jensen's inequality-induced bias term $A_n(u)$ in equation (18), which becomes more pronounced for "more variable" stochastic volatility models such as the two-factor volatility process as well as the macro-finance volatility specification. The results for Models 2 and 3 are similar. Finally, the numerical results show that the inference procedures perform similarly across the tuning parameter selections $u = \{1/20, 1/10, 1/5\}$.

6.2 *Bootstrap confidence intervals for spot measures*

We proceed by examining the properties of our new Laplace transform-based estimators and their associated bootstrap inference for the spot variance, covariance, correlation, and beta. To this end, we generate two processes $\{X_t, t \geq 0\}$ and $\{Y_t, t \geq 0\}$ in a setting reminiscent of the one in Reiss, Todorov, and Tauchen (2015). Specifically, the series are simulated according to the bivariate dynamics,

$$dX_t = \sqrt{V_t}\, dW_t + dL_t, \qquad dY_t = \beta_t\, dX_t + \sqrt{\tilde{V}_t}\, d\tilde{W}_t + d\tilde{L}_t, \tag{36}$$

$$dV_t = 0.03(1 - V_t)\, dt + 0.18\sqrt{V_t}\, dB_t, \qquad d\tilde{V}_t = 0.03(1 - \tilde{V}_t)\, dt + 0.18\sqrt{\tilde{V}_t}\, d\tilde{B}_t, \tag{37}$$

where $(W, \tilde{W}, B, \tilde{B})'$ is a vector of independent standard Brownian motions; L and $\tilde{L}$ are two pure-jump compound Poisson processes with intensity $\lambda = 4$ and jump sizes drawn from $N(0, 0.01)$, independent of each other, and of the Brownian motions. The spot variances V and $\tilde{V}$ in (36) are captured by square-root diffusion processes, which are used extensively in financial applications. Finally, for the process β, we let

$$d\beta_t = 0.03(1 - \beta_t)\, dt + 0.18\sqrt{\beta_t}\, dB_t^{\beta}, \tag{38}$$

with B^{β} being a Brownian motion, independent from the remaining Brownian motions in (36).

Since we examine the properties of spot measure estimators, which have a slower optimal rate of convergence than corresponding realized estimators, $\Delta_n^{-1/4}$ versus $\Delta_n^{-1/2}$, we consider slightly larger sample sizes $n = \{78, 288, 720, 1440\}$, which amounts to sampling every 20, 5, 2, and 1 minutes, respectively, for assets that are traded round-the-clock. Moreover, we fix $k_n = \lfloor \sqrt{n} \rfloor$ for the SLT estimator in (21), that is, its localizing window is set just below a selection implied by its optimal rate.[4] In addition, we consider a uniform kernel measure $W(du)$ in (24) and draw comparisons to spot estimators based on a single selection u. Specifically, we consider partitions of the range $[u_{\min}, u_{\max}] = [1/100, 1/5]$ with step length fixed at $1/100$; namely, $u_j = 1/100 + j/100$,

[4]Strictly speaking, our bootstrap procedures are only valid when $k_n/\sqrt{n} \to 0$. Hence, we consider $k_n = \lfloor \sqrt{n} \rfloor$ to be a simple rule-of-thumb selection. Furthermore, we assess the robustness of the bootstrap coverage to k_n in Figure 2.

$j = 0, 1, \ldots, 19$.[5] Finally, we assess the finite sample properties of our new SLT-based estimators against the TSRV, which as discussed in Remark 6, is an asymptotically efficient benchmark from the literature. As above, the simulations are based on 10,000 replications and 999 bootstrap draws for inference.

We focus on results for spot measure estimation and LG bootstrap inference. Table 2 reports the relative biases and RMSEs (from the relative bias) for different spot measure estimators. From these results, we first observe that all estimators converge as n increases, in line with the asymptotic results. Second, if implemented using large single index weights, $u \geq 1/10$, the spot estimators may perform poorly, having biases in excess of 10% for smaller samples and large RMSEs (see, e.g., the covariance and beta results). However, the results are accurate and much less sensitive if relying on a uniform weighting scheme, regardless of the implemented boundaries. Third, despite being asymptotically efficient, we observe that our SLT-based spot measure estimators perform better than the TLRV for most combinations of measures and sample size, especially for the recovery of spot variances and covariance. This illustrates a desirable combination of higher-order jump robustness and approximate asymptotic efficiency for our spot measure estimators.

When turning to the 95% coverage rates for the LG bootstrap in Table 3, we observe a slight tendency for the estimators to undercover when $n = 78$. However, for larger samples $n = \{288, 720, 1440\}$, the LG bootstrap provides accurate inference, especially for the correlation and beta estimates.

Finally, we examine the robustness of the coverage for the LG bootstrap to the selection of the localization window, k_n, in Figure 2. Interestingly, consistent with the requirement $k_n\sqrt{\Delta_n} \to 0$ for validity of the LG bootstrap in Theorems 8 and 10, the coverage is close to 95% for all sample sizes as long as k_n is not being selected too large. Naturally, the range of valid localization window selections depends on the sample size. When k_n is chosen too large, the local "variance of varianc" drives a wedge between the nominal 95% and empirical coverage rates (cf. Theorem 5). All-in-all, however, Figure 2 demonstrates that the LG bootstrap procedure is robust against window selection.

7. Empirical analysis

To illustrate the usefulness of our new spot measure estimators and their associated LG bootstrap inference procedures, we examine the volatility of, as well as the coherence between, futures contracts written on the S&P 500 (ES1) and 10-year US Treasuries (TY1) over the time span from January 2005 through December 2020. Specifically, using 2-minute log-returns from 8.00–22.00 CET, we estimate the end-of-day spot volatilities, correlation, and market beta to gauge the uncertainty of the two investments as well as the effectiveness of a fixed income hedge.[6] For each (full) trading day, the sampling

[5] The selections of $u_{\min}$ and $u_{\max}$ are inspired by Figure 1, which shows that the choices $u_{\min} = 1/100$ and $u_{\max} \leq 1/2$ generate approximately the same asymptotic efficiency as the TLRV estimator; see Remark 6.

[6] The data is obtained from `datastream`. Specifically, on each day, we truncate observations to the requisite interval and rely on last-tick interpolation to construct an equidistant 2-minute sampling grid from 1-minute observations.

TABLE 2. Relative bias and RMSE.

Relative bias and RMSE of spot measure estimators											
		bias, $\underline{u}=1/100$					RMSE, $\underline{u}=1/100$				
$\bar{u}=$	$n=$	$V(X)$	$V(Y)$	$C(X,Y)$	$\beta(X,Y)$	$\rho(X,Y)$	$V(X)$	$V(Y)$	$C(X,Y)$	$\rho(X,Y)$	$\beta(X,Y)$
1/50	78	0.0417	0.0427	0.0467	−0.0285	0.0026	0.5168	0.5090	0.6369	0.2912	0.3929
1/50	288	0.0461	0.0445	0.0464	−0.0161	0.0014	0.4092	0.3978	0.4922	0.2145	0.2905
1/50	720	0.0464	0.0454	0.0458	−0.0076	0.0033	0.3395	0.3088	0.3764	0.1549	0.2086
1/50	1440	0.0346	0.0335	0.0263	−0.0123	−0.0047	0.2932	0.2701	0.3177	0.1361	0.1803
1/10	78	0.0557	0.0586	0.0894	−0.0042	0.0293	0.5062	0.5190	0.6706	0.3062	0.4227
1/10	288	0.0446	0.0481	0.0544	−0.0078	0.0111	0.3871	0.3782	0.4733	0.2103	0.2837
1/10	720	0.0404	0.0398	0.0393	−0.0084	0.0030	0.3240	0.3076	0.3741	0.1649	0.2202
1/10	1440	0.0252	0.0269	0.0176	−0.0115	−0.0024	0.2648	0.2490	0.2976	0.1387	0.1823
1/5	78	0.0647	0.0800	0.0599	0.0079	0.0466	0.5239	0.5470	0.6311	0.3390	0.4560
1/5	288	0.0430	0.0539	0.0625	0.0076	0.0307	0.3812	0.3820	0.4874	0.2356	0.3143
1/5	720	0.0342	0.0393	0.0425	−0.0009	0.0130	0.3069	0.3018	0.3848	0.1852	0.2419
1/5	1440	0.0263	0.0261	0.0309	−0.0002	0.0082	0.2536	0.2472	0.3145	0.1532	0.1999
		bias					RMSE				
$u=$	$n=$	$V(X)$	$V(Y)$	$C(X,Y)$	$\beta(X,Y)$	$\rho(X,Y)$	$V(X)$	$V(Y)$	$C(X,Y)$	$\rho(X,Y)$	$\beta(X,Y)$
1/100	78	0.0472	0.0489	0.0577	−0.0217	0.0111	0.5156	0.5037	0.6310	0.2905	0.3981
1/100	288	0.0407	0.0421	0.0395	−0.0175	−0.0003	0.3863	0.3772	0.4628	0.2014	0.2720
1/100	720	0.0439	0.0415	0.0412	−0.0106	−0.0009	0.3418	0.3118	0.3823	0.1557	0.2075
1/100	1440	0.0379	0.0375	0.0322	−0.0097	−0.0024	0.3091	0.2752	0.3246	0.1313	0.1729
1/50	78	0.0482	0.0544	0.0623	−0.0218	0.0131	0.5228	0.5058	0.6430	0.2926	0.4016
1/50	288	0.0399	0.0421	0.0442	−0.0133	0.0038	0.3850	0.3756	0.4674	0.2031	0.2735
1/50	720	0.0443	0.0382	0.0382	−0.0100	−0.0015	0.3366	0.3104	0.3726	0.1553	0.2110
1/50	1440	0.0345	0.0315	0.0243	−0.0113	−0.0047	0.2935	0.2661	0.3087	0.1336	0.1747
1/10	78	0.0496	0.0678	0.1370	0.0240	0.0678	0.5207	0.5300	0.8211	0.3549	0.4733
1/10	288	0.0413	0.0535	0.0724	0.0061	0.0312	0.3790	0.3842	0.5179	0.2349	0.3160
1/10	720	0.0297	0.0351	0.0375	−0.0027	0.0116	0.3036	0.2994	0.3804	0.1823	0.2391
1/10	1440	0.0273	0.0269	0.0238	−0.0072	0.0013	0.2547	0.2456	0.3077	0.1518	0.1978
1/5	78	0.0572	0.0925	0.1334	0.0689	0.1203	0.5212	0.5914	0.8794	0.5194	0.6678
1/5	288	0.0488	0.0607	0.1381	0.0585	0.0867	0.3805	0.3955	0.6902	0.3768	0.4631
1/5	720	0.0266	0.0400	0.0815	0.0307	0.0510	0.2903	0.3070	0.5196	0.2883	0.3524
1/5	1440	0.0183	0.0246	0.0572	0.0229	0.0348	0.2400	0.2500	0.4067	0.2286	0.2776
		bias					RMSE				
	$n=$	$V(X)$	$V(Y)$	$C(X,Y)$	$\beta(X,Y)$	$\rho(X,Y)$	$V(X)$	$V(Y)$	$C(X,Y)$	$\rho(X,Y)$	$\beta(X,Y)$
TLRV	78	0.1738	0.1780	0.1769	−0.0308	0.0024	0.6132	0.5967	0.7333	0.2910	0.3928
TLRV	288	0.0967	0.1014	0.0991	−0.0158	0.0021	0.4152	0.4045	0.4992	0.1969	0.2644
TLRV	720	0.0785	0.0797	0.0776	−0.0127	−0.0017	0.3690	0.3432	0.4303	0.1579	0.2087
TLRV	1440	0.0768	0.0767	0.0809	−0.0036	0.0012	0.3488	0.2996	0.3878	0.1308	0.1724

Note: This table displays the relative bias and RMSE for various implementations of the new Laplace transform-based spot measure estimators in Section 5. Specifically, the upper panel provides results for different combinations of $\underline{u}=u_{\min}$ and $\bar{u}=u_{\max}$ using step length 1/100 and uniform kernel weights. The middle panel provides corresponding results for single index weights and different choices of u. The lower panel provides benchmark results using the TLRV estimator. The spot measures are localized around $\tau=1/2$ in all cases. The simulations are implemented with 10,000 replications.

Table 3. Spot measure coverage.

Local Gaussian bootstrap coverage rates for spot measures										
$n =$	$V(X)$	$V(Y)$	$C(X,Y)$	$\beta(X,Y)$	$\rho(X,Y)$	$V(X)$	$V(Y)$	$C(X,Y)$	$\beta(X,Y)$	$\rho(X,Y)$
	$(\underline{u}, \bar{u}) = (1/100, 1/10)$					$(\underline{u}, \bar{u}) = (1/100, 1/5)$				
78	91.89	91.69	92.48	94.46	94.96	92.43	92.22	92.99	95.80	95.56
288	92.26	92.19	92.67	93.82	94.68	92.43	92.65	93.01	95.15	95.25
720	93.39	93.32	93.45	94.34	94.45	93.88	93.52	93.63	95.44	94.96
1440	93.79	93.91	94.04	94.53	94.96	93.96	94.05	93.97	95.17	95.25
	$u = 1/100$					$u = 1/50$				
78	91.64	91.77	91.92	93.51	94.77	91.85	91.59	92.45	93.64	94.79
288	92.43	92.30	92.70	93.49	95.03	92.69	92.64	92.85	93.28	94.81
720	93.51	93.26	93.44	93.69	94.61	93.63	93.32	93.35	93.47	94.89
1440	93.87	94.06	93.86	93.60	94.36	93.72	93.86	93.67	93.59	94.77
	$u = 1/10$					$u = 1/5$				
78	92.07	92.13	92.89	95.80	95.73	91.87	92.51	91.55	95.06	94.53
288	92.25	92.57	92.73	95.22	95.03	92.09	92.67	93.01	96.09	95.56
720	93.46	93.58	93.84	95.15	95.23	93.14	93.27	93.88	95.73	95.43
1440	93.84	93.94	93.77	94.91	95.05	94.04	94.03	94.62	95.57	95.78

Note: Spot measure coverage. This table displays the local Gaussian bootstrap coverage rates for the new Laplace transform-based spot measure estimators in Section 5. The nominal level is 95%. Specifically, the upper panel provides coverage results for different combinations of $\underline{u} = u_{\min}$ and $\bar{u} = u_{\max}$ using step length 1/100 and uniform kernel weights. The two lower panels provide corresponding results for single index weights and different choices of u. The spot measures are localized around $\tau = 1/2$ in all cases. The simulations are implemented with 10,000 replications, each of which uses 999 bootstrap draws.

scheme implies that we have $n = 420$ observations and subsequently fix a local window of size $k_n = \lfloor 6n^{0.45} \rfloor = 90$. The estimators are implemented as in equations (24), (32), and (33) with tuning parameters $u_{\min} = 1/100$, $u_{\max} = 1/5$, step length 1/100, and a uniform kernel. In addition to the daily spot measure estimates, we use the LG bootstrap statistics $\mathcal{SV}^*_{n,\tau}$, $\mathcal{SV}^*_{n,C_\tau}$, $\mathcal{SV}^*_{n,\rho_\tau}$, and $\mathcal{SV}^*_{n,\beta_\tau}$, defined in Section 5, along with 999 bootstrap draws to compute corresponding 2.5% and 97.5% quantiles along with the bootstrap standard deviation, which will be useful for our unconditional analysis of hedging efficacy and our forecasting exercise, respectively. Before proceeding to the latter, however, Table 4 provides summary statistics of the estimated spot measures, their bootstrap quantiles, and standard deviations as well as daily log-returns on the futures contracts themselves.

There are several noteworthy observations in Table 4. First, we find, not surprisingly, that the average spot volatility on ES1 is 3–4 times larger than for TY1. More interestingly, however, the persistence for ES1, which is measured by its first-order autoregressive coefficient (AR(1)), is almost double that for TY1, hinting that stock market volatility is more predictable than 10-year Treasury bond volatility. Second, the average correlation between the two assets is negative, consistent with fixed income being viewed as an important hedge for equity investments. This feature is corroborated by the average 95% bootstrap confidence interval, which suggests that the spot correlation is significantly negative. However, the bootstrap standard deviation for these estimates indicate that there is high degree of uncertainty surrounding the exact magnitude of the coherence. In fact, the time-series average bootstrap standard deviation for the spot correlation measure is higher than the corresponding uncertainty measures for the two spot

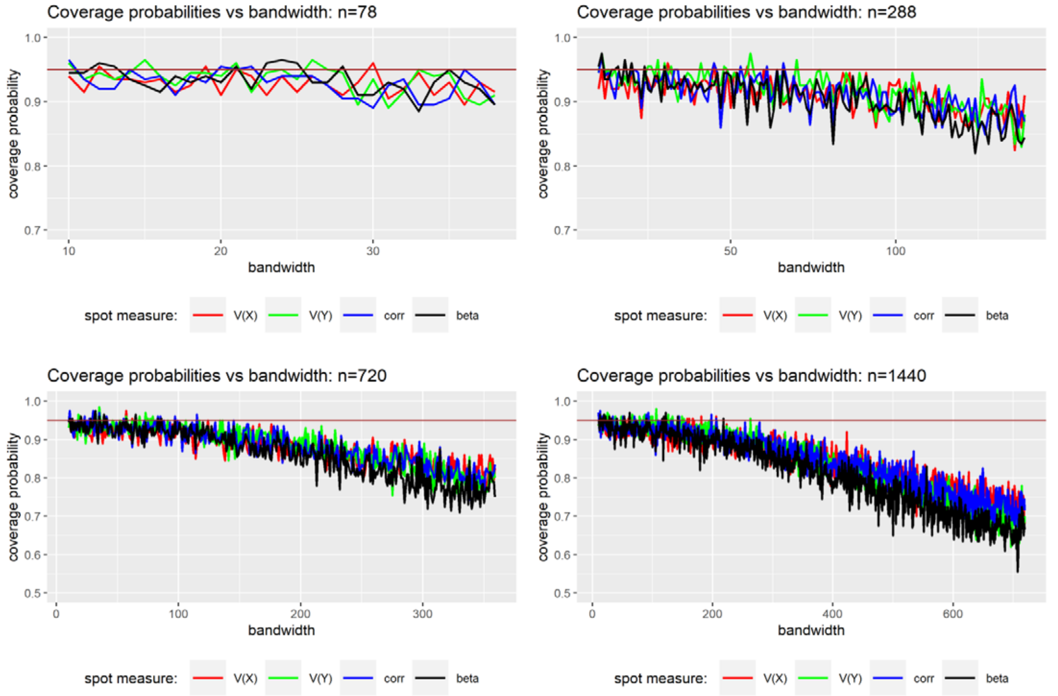

FIGURE 2. Coverage probability and the bandwidth. This picture examines the robustness of the coverage for the new Laplace transform-based spot measure estimators to the bandwidth parameter, k_n, using local Gaussian bootstrap inference. Specifically, the upper left depict a scenario where $n = 78$ and $k_n \in [10, 39)$; upper right where $n = 288$ and $k_n \in [10, 144)$; lower left where $n = 720$ and $k_n \in [10, 360)$; and lower right where $n = 1440$ and $k_n \in [10, 720)$. The spot measures are estimated using parameters $u_{\min} = 1/100$, $u_{\max} = 1/5$ with step length $1/100$ and a uniform kernel. Moreover, they are localized around $\tau = 1/2$ in all cases. The nominal level of the coverage is 95%. The simulations are implemented with 10,000 replications, each of which uses 999 bootstrap draws.

volatilities and the spot market beta. Finally, while the average spot market beta is negative, the average 95% bootstrap confidence interval suggests that it is insignificantly different from zero, indicating that balanced portfolios with a constant exposure to a fixed income hedge may not necessarily perform well in all stock market environments.[7]

7.1 *Assessing hedging performance*

We assess the efficiency of having adopted a fixed income futures (TY1) hedge for S&P 500 futures investments (ES1) on the 20 *worst* equity trading days from 2005 through 2020 in Figure 3. Specifically, we condition on the 20 days with the lowest daily ES1 return and depict our spot estimates of volatility, correlation, and beta along with their LG

[7]An example of a constant exposure portfolio is the (in)famous 60–40% portfolio of stocks and bonds, which has been popularized by the mutual fund Vanguard and remains an important benchmark for many passive investors.

TABLE 4. Summary statistics.

Summary statistics for risk measures								
	Mean	StDev	Skewness	Kurtosis	AR(1)	$\mathcal{Q}(2.5)$	$\mathcal{Q}(97.5)$	$\mathcal{BV}^*$
ES1	0.0296	1.2460	−0.3413	18.7692	−0.1140	−2.6064	2.1926	–
TY1	0.0130	0.3497	0.1264	8.1748	−0.0306	−0.6979	0.6980	–
V(ES1)	1.0227	0.8936	4.1386	29.3498	0.8135	0.8827	1.1627	0.6809
V(TY1)	0.3030	0.1775	7.4642	156.9589	0.4275	0.2556	0.3504	0.2272
corr	−0.2420	0.2228	0.0170	3.0637	0.5786	−0.4267	−0.0574	0.8996
beta	−0.0720	0.0793	0.9724	11.5279	0.3721	−0.1540	0.0100	0.3968

Note: This table displays summary statistics for log-returns on S&P 500 and 10-year Treasury bond futures contracts (ES1 and TY1), end-of-day spot volatility estimates as well as the estimates of the corresponding spot correlation and spot market beta. Using 2-minute intraday observations, the spot measures are estimated as described in Sections 5 and 6.2, that is, with tuning parameters $u_{\min} = 1/100$, $u_{\max} = 1/5$, step length $1/100$, and a uniform kernel. Moreover, a bandwidth $k_n = 6\lfloor \Delta_n^{0.45} \rfloor$ is applied. Standard unconditional summary statistics are provided along with first-order autoregressive coefficients, AR(1), 2.5% and 97% quantiles of the variables, and the average bootstrap standard deviation from daily estimates of the (local Gaussian) bootstrap distributions, $\mathcal{BV}^*$. Whereas the quantiles for ES1 and TY1 are standard, the quantiles for the spot measures are captured by the average over daily 2.5% and 97% bootstrap quantiles. The sample period spans from January 2005 through December 2020. Finally, the returns and spot volatility measures are quoted in daily percentages.

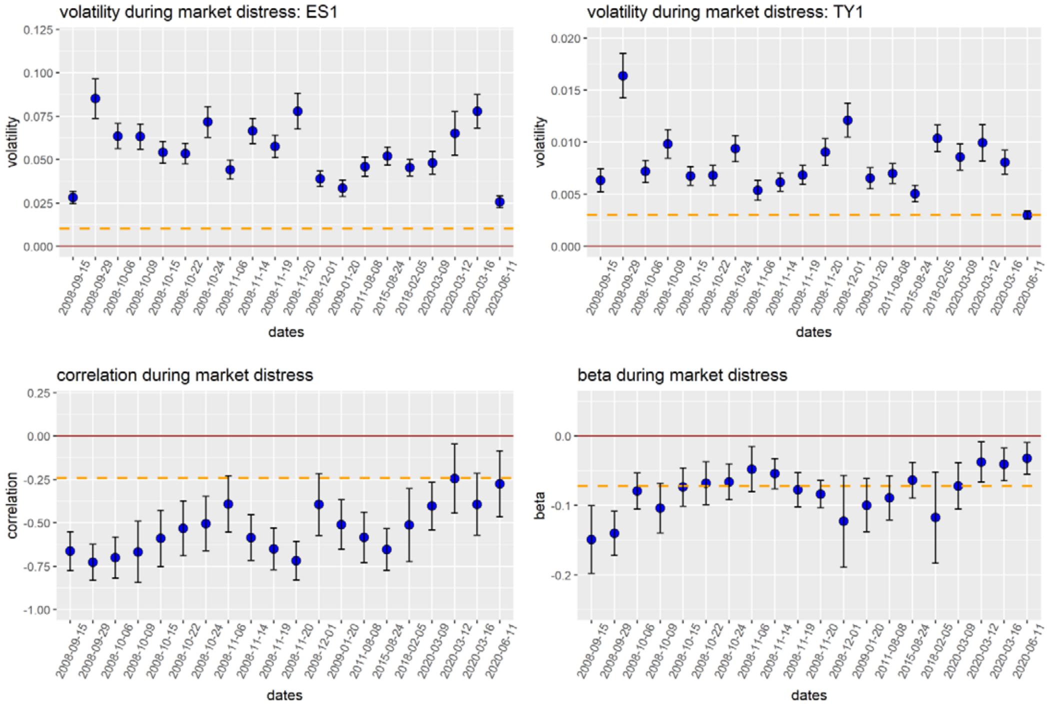

FIGURE 3. Risk measures during market distress. This picture displays end-of-day spot volatility, correlation, and market beta estimates together with associated 95% confidence intervals based on the local Gaussian bootstrap for the 20 days with the *worst* daily return on S&P 500 futures contracts (ES1). Moreover, the dashed orange line provide the average spot measure estimate over the full sample from January 2005 through December 2020. The estimates of the spot measures are implemented as described in Table 4.

bootstrap confidence intervals. This allows not only to quantify risk on those days, but also the uncertainty surrounding popular risk measures.

Interestingly, we observe that 12/20 of the worst stock market days occur during the last 4 months of 2008, reflecting the global financial crisis, and 4/20 during March and June 2020, reflecting the COVID-19 pandemic-induced stock market sell-off.[8] More specifically, if we consider the spot correlation and market beta results during these episodes, they reveal anatomies of two different crises. In particular, while the correlation between ES1 and TY1 during the global financial crisis was significantly below its unconditional mean, it was insignificantly different from it during the COVID-19 pandemic sell-off. Moreover, the spot betas was significantly below its mean on key days during the financial crisis, for example, during the decline on September 15, 2008, with Lehman Brothers filing for bankruptcy. In contrast, after March 9, 2020, the spot market beta is significantly *above* its unconditional mean. This asymmetry suggests that static balanced portfolios have enjoyed substantial diversification benefits during 2008 and suffered from a lack of fixed-income protection during 2020.

This pattern is corroborated in Figure 4, where we plot the ES1 and TY1 indices during 2008 and 2020 in the top panels, and we depict the frequency (of trading days) at which the spot correlation and beta is significantly above, respectively, below their full sample averages in the bottom panels.[9]

Interestingly, we observe that the correlation (beta) is below its sample average on more than 80% (60%) of the days during 2008, with TY1 increasing steadily during the last 4 months of the year. In contrast, TY1 is essentially flat after March 9, 2020, and the beta is significantly above its unconditional average on more than 30% of the trading days, including days with massive equity sell-offs, as seen in Figure 3. Hence, these patterns, which are only revealed by our spot measure estimators and associated LG bootstrap inference procedures, thus call for a dynamic and disciplined approach to stock-bond allocation in balanced portfolios. Specifically, they illustrate that in order to have achieved a 2008 level of fixed income protection for equity investments during 2020, the relative exposure to fixed income products must have been substantially larger.

7.2 *Forecasting risk measures*

In addition to providing useful information about the magnitudes and significance of key risk measures in an unconditional, in-sample exercise, we continue assessing the quality of our spot measure estimators and associated LG bootstrap procedures in an out-of-sample setting. To this end, we adopt the HAR-Q framework from Bollerslev, Patton, and Quaedvlieg (2016). While the latter apply their methodology to standard realized variance (and realized kernel) estimates, one may directly adapt their framework to

[8]The remaining 4 days similarly have intuitive explanations; 2009-01-20 was the inauguration day for Barack Obama, which exhibited a stock sell-off that was widely credited to a continued lack of confidence in the failing economy; 2011-08-08 had fearful investors reacting strongly to Standard & Poor's downgrade of United States' credit rating from AAA; 2015-08-24 saw the occurrence—the now famous—"flash crash" episode; and 2018-02-05 simultaneously exhibited a large stock sell-off and a massive spike in VIX, which were associated with an inflation scare among investors.

[9]We have utilized the LG bootstrap confidence intervals to determine significance as in Figure 3.

FIGURE 4. Hedging efficacy. This picture provides perspectives on the cross-hedging performance for a portfolio consisting of S&P 500 and 10-year Treasury bond futures contracts (ES1 and TY1). Specifically, the upper left and right quadrants show the performance of the two assets during 2008 and 2020, respectively. The lower left quadrant shows the frequency at which the estimated end-of-day spot correlation is significantly above (red, left), respectively, below (green, right) the average (over the full sample) spot correlation in a given year using the local Gaussian bootstrap to determine the significance level (i.e., quantiles). The lower right quadrant provides corresponding results for the spot market beta. The sample period spans from January 2005 through December 2020.

spot measure forecasting as long as we have a daily estimate of their requisite asymptotic variance. In our case, we obtain these by the LG bootstrap.

Specifically, let $\mathcal{R}_t$ denote some spot risk measure (either volatility, correlation, or beta) and $\mathcal{BV}_t^*$ be its LG bootstrap standard deviation. Then we will examine forecasting models of the form:

$$\begin{aligned}\overline{\mathcal{R}}_{t+1,-h} = \beta_0 + \beta_1 \overline{\mathcal{R}}_{t,1} + \beta_2 \overline{\mathcal{R}}_{t,5} + \beta_3 \overline{\mathcal{R}}_{t,21} \\ + \mathcal{BV}_t^* (\gamma_1 \overline{\mathcal{R}}_{t,1} + \gamma_2 \overline{\mathcal{R}}_{t,5} + \gamma_3 \overline{\mathcal{R}}_{t,21}) + \varepsilon_{t+1,-h},\end{aligned} \tag{39}$$

where $\overline{\mathcal{R}}_{t,h} = h^{-1} \sum_{i=0}^{h-1} \mathcal{R}_{t-i}$ for $h \geq 1$ and $\overline{\mathcal{R}}_{t,h} = |h|^{-1} \sum_{i=0}^{|h|-1} \mathcal{R}_{t+i}$ for $h < 0$ are averages of the spot measure estimates over $|h|$ days. This framework nests several interesting dynamic forecasting models. For example, if we set $h = 1$ and fix $\beta_2 = \beta_3 = \gamma_1 = \gamma_2 = \gamma_3 = 0$, the model reduces to an AR(1) process. By subsequently relaxing the restriction $\gamma_1 = 0$, the model facilitates an adjustment of attenuation bias due to potential measurement errors in $\mathcal{R}_t$. Similarly, by imposing the restrictions $\gamma_1 = \gamma_2 = \gamma_3 = 0$, we recover the popular HAR model of Corsi (2009), thereby accommodating long memory-style variation in $\mathcal{R}_t$. Finally, the HAR-Q models with an attenuation adjustment for either the first term or all three are recovered by relaxing restrictions on γ_1, γ_2, and γ_3.

The HAR-Q framework provides a simple, yet powerful setting to assess the quality of our risk measure estimates by explicitly accounting for attenuation bias due to measurement errors. That is, the relative forecasting prowess of dynamics models with and without the bias correction speaks to the quality of both our risk measure *and* its asymptotic variance estimate. Hence, we leverage our new SLT-based spot measure estimators and LG bootstrap procedures to compute their asymptotic variances to evaluate: (i) whether the spot measures require corrections for attenuation bias; (ii) whether the attentuation bias correction contains significant predictive information. Collectively, this exercise provides an out-of-sample perspective on the quality of our procedures.

Table 5 provides in-sample estimates of these five nested model specifications for the spot volatility, correlation, and market beta measures. There are several interesting results. First, consistent with the AR(1) coefficients in Table 4, the ES1 spot volatility series is by far the most predictable, judging by the adjusted R^2. Second, the attenuation bias adjustment using the bootstrap standard deviation is very effective for the AR(1) model, but provides smaller gains in R^2 for the baseline HAR structure. The HAR improvements, however, are still nontrivial for the spot correlation and beta series. Third, the HAR models, with and without attenuation bias adjustments, perform substantially better than the corresponding AR(1) models, indicating that long memory is prevalent in the risk measures. Once the latter is controlled for, this partially corrects the time-varying attenuation bias, whose adjustment only generates smaller gains. Taken together, the results suggests that estimation errors are present in the risk measures, but the long memory signal is dominating their time variation.

To elaborate on these results, Table 6 displays root mean squared forecast errors (RMSFEs) from an out-of-sample exercise. Specifically, we consider forecast horizons $h = 1$ and $h = 21$ (monthly), initialize the models using the first 250 trading days, and apply an expanding window of observations. Moreover, we use the 10% model confidence set (MCS) from Hansen, Lunde, and Nason (2011) to determine which models provide the best forecasts. The results are clear; the HAR models are significantly better than the AR(1) models for all spot measure series. The HAR-Q models, using the LG bootstrap standard deviation, seem to add value over the standard HAR model for the spot volatility on TY1 as well as the spot correlation and market beta, indicating useful predictive information. However, the differences are only significant for the monthly spot correlation forecasts.

8. Conclusion

In this paper, we study fixed-span inference for the RLT using bootstrap procedures in a general semimartingale setting. Despite the RLT having features suggesting that wild bootstrap methods may be appropriate, such as its summands being conditionally uncorrelated and heteroskedastic, we show that existing bootstrap procedures provide inconsistent inference. Hence, as a solution, we propose a local Gaussian (LG) bootstrap,

Table 5. HAR-Q models.

	In-sample bootstrap HAR-Q model analysis									
	AR	AR-Q	HAR	HAR-Q	HAR-QF	AR	AR-Q	HAR	HAR-Q	HAR-QF
	ES1 volatility					TY1 volatility				
β_0	0.0019	0.0008	0.0007	0.0001	0.0006	0.0017	0.0009	0.0004	0.0001	0.0006
	(7.6667)	(1.6087)	(2.7489)	(0.3438)	(1.9182)	(7.8224)	(4.4948)	(3.6240)	(0.6603)	(3.3272)
β_1	0.8135	0.9421	0.3790	0.4582	0.5297	0.4275	0.7312	0.1083	0.2626	0.1996
	(31.011)	(14.953)	(6.4030)	(8.6892)	(8.2578)	(5.9474)	(9.6172)	(2.5440)	(3.9811)	(3.6271)
β_2	–	–	0.4640	0.4678	0.3148	–	–	0.2689	0.2547	0.1538
			(5.7059)	(5.6704)	(4.9957)			(2.7549)	(2.3841)	(2.4245)
β_3	–	–	0.0931	0.0710	0.1029	–	–	0.5001	0.4629	0.4419
			(1.7588)	(1.2241)	(2.0836)			(4.1884)	(4.4384)	(6.5598)
γ_1	–	−4.6001	–	−2.4333	−9.8399	–	−50.324	–	−22.124	−37.684
		(−1.8950)		(−1.2501)	(−2.3707)		(−4.5640)		(−2.9390)	(−4.4017)
γ_2	–	–	–	–	12.802	–	–	–	–	55.346
					(1.7974)					(0.8191)
γ_3	–	–	–	–	−2.8047	–	–	–	–	14.079
					(−0.4470)					(0.1957)
Adj. R^2	0.6616	0.6681	0.7129	0.7146	0.7181	0.1824	0.2156	0.3137	0.3194	0.3254

(*Continues*)

TABLE 5. *Continued.*

In-sample bootstrap HAR-Q model analysis										
	AR	AR-Q	HAR	HAR-Q	HAR-QF	AR	AR-Q	HAR	HAR-Q	HAR-QF
	Correlation					beta				
β_0	−0.1024	−0.1189	−0.0251	−0.0390	−0.0367	−0.0454	−0.0389	−0.0105	−0.0092	−0.0091
	(−23.097)	(−21.993)	(−5.3233)	(−7.1860)	(−6.2840)	(−21.905)	(−19.521)	(−4.7439)	(−4.1247)	(−4.0384)
β_1	0.5783	0.4319	0.1874	0.1409	0.1473	0.3712	0.4408	0.0546	0.1116	0.1139
	(32.660)	(19.871)	(9.0201)	(6.5466)	(6.6739)	(14.734)	(20.498)	(2.6096)	(5.0691)	(4.7221)
β_2	–	–	0.3985	0.3568	0.3568	–	–	0.3483	0.3268	0.3405
			(11.324)	(10.076)	(10.009)			(7.1931)	(6.7428)	(7.2533)
β_3	–	–	0.3107	0.3002	0.3022	–	–	0.4518	0.4226	0.4082
			(8.9447)	(8.8786)	(8.6976)			(9.2066)	(8.5800)	(8.2919)
γ_1	–	−0.7731	–	−0.4085	−0.6007	–	−0.5498	–	−0.2925	−0.2848
		(−11.704)		(−7.0186)	(−3.9473)		(−5.0547)		(−3.6904)	(−2.5198)
γ_2	–	–	–	–	0.2808	–	–	–	–	−0.1939
					(1.0840)					(−1.0565)
γ_3	–	–	–	–	−0.0426	–	–	–	–	0.2479
					(−0.2119)					(1.6698)
Adj. R^2	0.3341	0.3645	0.4463	0.4540	0.4540	0.1374	0.1695	0.2726	0.2811	0.2812

Note: This table provides in-sample estimates of nested HAR-Q model specifications. Specifically, from the representation in (39), an AR(1) model with and without an attenuation bias adjustment are considered (labeled AR, respectively, AR-Q) together with a HAR model and HAR-Q models with attenuation bias adjustments for either the first or all three terms, with the latter being denoted by HAR-QF. In addition to coefficient estimates, t-statistics based the Andrews (1991) standard errors using the Parzen kernel are reported in parentheses. The sample period spans from January 2005 through December 2020.

Table 6. HAR-Q model forecasting.

	Out-of-sample bootstrap HAR-Q model analysis									
	Daily					Monthly				
	AR	AR-Q	HAR	HAR-Q	HAR-QF	AR	AR-Q	HAR	HAR-Q	HAR-QF
V(ES1)	0.5423	0.5409	**0.5011**⋆	0.5080⋆	0.5195⋆	0.5163	0.5154	**0.4731**⋆	0.4798⋆	0.4896⋆
V(TY1)	0.1675	0.1624	0.1514⋆	**0.1506**⋆	0.1510⋆	0.1003	0.0925	0.0713⋆	0.0701⋆	**0.0700**⋆
corr	18.347	17.937	16.684⋆	**16.585**⋆	16.631⋆	12.590	12.172	10.331	**10.238**⋆	10.268⋆
beta	7.4925	7.3930	6.8644⋆	**6.8420**⋆	6.8845⋆	4.1630	4.0492	3.2340⋆	**3.2168**⋆	3.2286⋆

Note: This table provides forecasting results for different nested HAR-Q model specifications. Specifically, from the representation in (39), an AR(1) model with and without an attenuation bias adjustment are considered (labeled AR, respectively, AR-Q) together with a HAR model and HAR-Q models with attenuation bias adjustments for either the first or all three terms, with the latter being denoted by HAR-QF. The table reports RMSFE (multiplied by 100) for both 1 day volatility forecasts and forecasts of the average volatility over a month (21 days). The model estimates and forecasts are initialized using 250 observations and reestimated using an expanding window. While we report RMSFE in the table, the star (⋆) indicate that the MSFE belongs to the 10% model confidence set (MCS) from Hansen, Lunde, and Nason (2011). The MCS is implement using the `T-max` statistic. The sample period spans from January 2005 through December 2020.

establish its first-order asymptotic validity, and use Edgeworth expansions to show that the LG bootstrap inference achieves second-order asymptotic refinements.

We broaden the scope of our LG bootstrap by introducing new estimators for the spot variance as well as the spot covariance, correlation, and beta between two semimartingales that are based on the Laplace transform, and we adapt the inference procedures to the requisite scenarios. We establish the central limit theory for the estimators, demonstrating that these can achieve the optimal rate of convergence, $\Delta_n^{-1/4}$. Moreover, first-order asymptotic validity of the LG bootstrap is established at a near-optimal rate. Unlike previous studies of bootstrap inference in the high-frequency econometrics literature, we provide both pointwise and uniform (bootstrap) limit theory for the RLT and the spot Laplace transform (SLT), which represent random processes. Not only does this add substantial complexity to the first-order asymptotic analysis, it makes the higher-order analysis particularly novel. The uniform results are necessary for the design of, and inference for, our spot (co)variance estimators, which are constructed by transforming the SLT function and evaluating it over a compact support.

A simulation study shows that the LG bootstrap outperforms existing feasible inference theory and alternative wild bootstrap methods, and it demonstrates that our new spot measure estimators and inference procedures are very accurate. Moreover, we illustrate the use of the new methods by examining the volatility of, as well as the coherence between, stocks and bonds from January 2005 through December 2020, showing that bonds have provided an effective hedge during the global financial crisis in 2008, but lacked protective ability during the COVID-19 pandemic stock sell-off. Finally, our (bootstrap) methods provide useful information for risk measure forecasting.

Appendix A: Additional assumptions

Assumption B′. The volatility, σ_{jt}, $j = 1, 2$ are Itô semimartingales, defined by

$$\sigma_{1t} = \sigma_{10} + \int_0^t \tilde{a}_{1s}\, ds + \int_0^t v_{1s}\, dW_{1s} + \int_0^t v'_{1s}\, dW_{2s}$$

$$
\begin{aligned}
&+\int_0^t v''_{1s}\,dW'_s+\int_0^t\int_{\mathbb{R}}\delta'_1(s-,x)\tilde{\mu}'_1(ds,dx),\\
\sigma_{2t}={}&\sigma_{20}+\int_0^t\tilde{a}_{2s}\,ds+\int_0^t v_{2s}\,dW_{1s}+\int_0^t v'_{2s}\,dW_{2s}+\int_0^t v''_{2s}\,dW'_s+\int_0^t v'''_{2s}\,dW''_s\\
&+\int_0^t\int_{\mathbb{R}}\delta'_2(s-,x)\tilde{\mu}'_2(ds,dx),
\end{aligned}
$$

where (W', W'') is a 2-dimensional standard Brownian motion, independent of $\mathbf{W}$, $\tilde{\mu}'_1$, $\tilde{\mu}'_2$, are compensated homogeneous Poisson measures with Lévy measure $dt\otimes\nu'_1(dx)$, $dt\otimes\nu'_2(dx)$, respectively, having arbitrary dependence with μ_1 and μ_2, and $\delta'_1(t,x)$, $\delta'_2(t,x)$ are mappings from $\mathbb{R}_+\times\mathbb{R}\to\mathbb{R}$, and are càdlàg in t. In addition, for every $t, s > 0$ and some $\iota > 0$, it is required that

$$
\begin{aligned}
&\mathbb{E}\biggl(|a_{jt}|^{3+\iota}+|\tilde{a}_{jt}|^2+|\sigma_{jt}|^{3+\iota}+|v_{jt}|^{3+\iota}+\bigl|v'_{jt}\bigr|^{3+\iota}+\int_{\mathbb{R}}\bigl|\delta'_j\bigr|^{3+\iota}\nu'_j(dx)\biggr)<C,\\
&\mathbb{E}\biggl(|a_{jt}-a_{js}|^2+|v_{jt}-v_{js}|^2+|\rho_t-\rho_s|^2+\bigl|v'_{jt}-v'_{js}\bigr|^2\\
&\quad+\int_{\mathbb{R}}\bigl(\delta'_j(t,x)-\delta'_j(s,x)\bigr)^2\nu'_j(dx)\biggr)<C|t-s|,
\end{aligned}
$$

for $j = 1, 2$, where $C > 0$ is some constant that does not depend on t and s.

Appendix B: Macro finance model parameters

The parameter values for Model 3 are borrowed from the estimates in Campbell et al. (2018, Table 1):

$$
\boldsymbol{\mu}=\begin{bmatrix}0.221\\-0.016\\0.155\\0.001\\0.194\\0.147\end{bmatrix},\qquad
A=\begin{bmatrix}
0.041 & 0.335 & -0.042 & -0.810 & 0.010 & -0.051\\
-0.002 & 0.441 & 0.005 & -0.021 & 0.004 & 0.001\\
0.130 & 0.674 & 0.961 & -0.399 & -0.001 & -0.024\\
0.002 & -0.084 & 0.001 & 0.948 & 0.001 & -0.001\\
-0.293 & 11.162 & -0.118 & 4.102 & 0.744 & 0.175\\
0.069 & 2.913 & -0.017 & -0.253 & -0.004 & 0.932
\end{bmatrix},
$$

and $\boldsymbol{\Sigma}$ is their unscaled covariance matrix subject to a small adjustment to ensure positive definiteness:[10]

$$
\boldsymbol{\Sigma}=\begin{bmatrix}
0.0609 & 0.0089 & -0.0149 & 0.0092 & -0.0103 & -0.0032\\
0.0089 & 0.1423 & -0.1697 & 0.1328 & -0.1849 & -0.0011\\
-0.0149 & -0.1697 & 0.4992 & -0.4087 & 0.6346 & -0.0794\\
0.0092 & 0.1328 & -0.4087 & 0.4770 & -0.6794 & 0.1209\\
-0.0103 & -0.1849 & 0.6346 & -0.6794 & 1.1905 & -0.2276\\
-0.0032 & -0.0011 & -0.0794 & 0.1209 & -0.2276 & 0.1336
\end{bmatrix},
$$

Finally, we set the initial value as $\boldsymbol{X}_0 = [\log(100)\ 0.2\ -0.03\ 0.111\ -0.113\ 0.004]$.

[10] For the adjustment, we simply replace the negative eigenvalues with the smallest positive eigenvalue.

Appendix C: The failure of standard wild bootstrap procedures

This section examines the asymptotic properties of two wild bootstrap procedures for the RLT. Specifically, we show that adaptations of the Gonçalves and Meddahi (2009) as well as and Wu (1986) and Liu (1988) bootstrap procedures to the present setting deliver inconsistent inference.

Since the sequence $(\xi(u)_i^n)_{i=1}^n$ is uncorrelated and heteroskedastic, the wild bootstrap inference procedure represents a natural alternative to the feasible limit theory in Section 2. This section adapts the procedures by Gonçalves and Meddahi (2009) as well as Wu (1986) and Liu (1988), labeled the GM and WL bootstrap, respectively, and studies their asymptotic (in)validity.

GM bootstrap

Following Gonçalves and Meddahi (2009), we define wild bootstrap pseudo observations $(\xi(u)_i^{n*})_{i=1}^n$ as

$$\xi(u)_i^{n*} = \xi(u)_i^n \eta_i^*. \tag{C.1}$$

Then, as it trivially follows that $\mathbb{E}^*(\mathrm{RLT}_n^*(u)) = \mu_1^* \,\mathrm{RLT}_n(u)$ and

$$C_n^*(u, v) = \big(\mu_2^* - (\mu_1^*)^2\big)\Delta_n \sum_{i=1}^n \xi(u)_i^n \xi(v)_i^n,$$

we use these moment results to formally establish that the GM bootstrap fails to consistently estimate the covariance function of the RLT, $\int_0^T F(\sqrt{uc_s}, \sqrt{vc_s})\, ds$ for some $u, v \in \mathbb{R}_+$.

Proposition 3. *Suppose Assumptions A and B hold, and that $\xi(u)_i^{n*}$ is generated as in (C.1). Then it follows that*

$$C_n^*(u, v) \xrightarrow{\mathbb{P}} \big(\mu_2^* - (\mu_1^*)^2\big) \int_0^T G(\sqrt{uc_s}, \sqrt{vc_s})\, ds,$$

as $\Delta_n \to 0$, with

$$G(x, y) \equiv \frac{e^{-(x+y)^2} + e^{-(x-y)^2}}{2}, \quad \text{for } x, y \in \mathbb{R}_+.$$

Note that by (4) and Proposition 3, we may write

$$G(x, y) = F(x, y) + e^{-x^2-y^2}, \quad \text{for } x, y \in \mathbb{R}_+.$$

Hence, there exist no choices of μ_1^* and μ_2^* such that

$$\big(\mu_2^* - (\mu_1^*)^2\big) \int_0^T G(\sqrt{uc_s}, \sqrt{vc_s})\, ds = \int_0^T F(\sqrt{uc_s}, \sqrt{vc_s})\, ds$$

holds true, showing that the GM bootstrap inference is inconsistent. The main reason for this inconsistency is that the bootstrap observations, defined by (C.1), are not centered appropriately.

WL bootstrap

To alleviate bias issues for wild bootstrap procedures, Wu (1986) and Liu (1988) propose to augment the resampling scheme with a delete-one jackknife bias correction. Hence, following their analyses, we define wild bootstrap pseudo observations $(\xi(u)_i^{n*})_{i=1}^n$ as

$$\xi(u)_i^{n*} = \frac{1}{n}\sum_{i=1}^n \xi(u)_i^n + \left(\xi(u)_i^n - \frac{1}{n}\sum_{i=1}^n \xi(u)_i^n\right)\eta_i^*. \tag{C.2}$$

That is, in contrast to (C.1), the WL bootstrap resampling scheme in (C.2) centers the observations around the sample mean. As above, it is straightforward to show that

$$\mathbb{E}^*\big(\mathrm{RLT}_n^*(u)\big) = \mathrm{RLT}_n(u) + \Delta_n \sum_{i=1}^n \left(\xi(u)_i^n - \frac{1}{n}\sum_{i=1}^n \xi(u)_i^n\right)\mu_1^* \quad \text{and}$$

$$\begin{aligned} C_n^*(u,v) &= \big(\mu_2^* - (\mu_1^*)^2\big)\Delta_n \sum_{i=1}^n \xi(u)_i^n \xi(v)_i^n \\ &\quad - \big(\mu_2^* - (\mu_1^*)^2\big)\frac{\Delta_n}{n}\left(\sum_{i=1}^n \xi(u)_i^n\right)\left(\sum_{i=1}^n \xi(v)_i^n\right), \end{aligned}$$

which is then used to establish the following inconsistency result.

Proposition 4. *Suppose Assumptions A and B hold, and that $\xi(u)_i^{n*}$ is generated as in (C.2). Then, as $\Delta_n \to 0$, it follows that*

$$\begin{aligned} C_n^*(u,v) \xrightarrow{\mathbb{P}} &\big(\mu_2^* - (\mu_1^*)^2\big)\int_0^T G(\sqrt{uc_s}, \sqrt{vc_s})\,ds \\ &- \frac{\big(\mu_2^* - (\mu_1^*)^2\big)}{T}\left(\int_0^T e^{-uc_s}\,ds\right)\left(\int_0^T e^{-vc_s}\,ds\right). \end{aligned}$$

Note that, for the WL bootstrap, we have

$$\frac{1}{T}\left(\int_0^T e^{-uc_s}\,ds\right)\left(\int_0^T e^{-vc_s}\,ds\right) = \int_0^T e^{-(u+v)c_s}\,ds \tag{C.3}$$

if and *only* if the volatility is constant, that is,

$$\sigma_t = \sigma > 0. \tag{C.4}$$

In this special case, Proposition 4 demonstrates the WL bootstrap can achieve consistent inference for the RLT by selecting the external variables $(\mu_2^* - (\mu_1^*)^2) = 1$ (i.e., $\mathbb{V}^*(\eta^*) = 1$), similar to the recommendations in Liu (1988). More generally, however, when allowing for stochastic volatility and leverage effects in Assumption B, the equality in (C.3) no longer holds, implying that there exist no choice of external variables that will render the bootstrap procedure consistent.

References

Aït-Sahalia, Yacine, Jianqing Fan, Roger J. A. Laeven, Christina D. Wang, and Xiye Yang (2017), "Estimation of the continuous and discontinuous leverage effects." *Journal of the American Statistical Association*, 112, 1744–1758. [1064]

Aït-Sahalia, Yacine and Jean Jacod (2014), *High-Frequency Financial Econometrics*. Princeton University Press. [1060]

Aït-Sahalia, Yacine and Jean Jacod (2009), "Testing for jumps in a discretely observed process." *Annals of Statistics*, 37, 184–222. [1060, 1062]

Alvarez, Alexander, Fabien Panloup, Monique Pontier, and Nicolas Savy (2012), "Estimation of instantaneous volatility." *Statistical Inference for Stochastic Processes*, 15, 27–59. [1073]

Andersen, Torben G., Tim Bollerslev, Francis X. Diebold, and Paul Labys (2001), "The distribution of exchange rate volatility." *Journal of the American Statistical Association*, 96, 42–55. [1060]

Andersen, Torben G., Tim Bollerslev, Francis X. Diebold, and Paul Labys (2003), "Modeling and forecasting realized volatility." *Econometrica*, 71, 579–625. [1060]

Andersen, Torben G., Nicola Fusari, Viktor Todorov, and Rasmus T. Varneskov (2019), "Option panels in pure-jump settings." *Econometric Theory*, 35, 901–942. [1060]

Andersen, Torben G., Tim Bollerslev, Peter F. Christoffersen, and Francis X. Diebold (2013), "Financial risk measurement for financial risk management." In *Handbook of the Economics of Finance* (G. Constantinides, M. Harris, and R. Stulz, eds.), 1127–1220, Elsevier, North Holland. [1060]

Andersen, Torben G. and Luca Benzoni (2012), "Stochastic volatility." In *Encyclopedia of Complexity and Systems Science* (Roberts A. Meyers, ed.). Springer. Forthcoming. [1064]

Andrews, Donald W. K. (1991), "Heteroskedasticity and autocorrelation consistent covariance matrix estimation." *Econometrica*, 59 (3), 817–858. [1094]

Bandi, Federico M. and Roberto Reno (2016), "Price and volatility co-jumps." *Journal of Financial Economics*, 119, 107–146. [1062]

Bandi, Federico M. and Roberto Reno (2018), "Nonparametric stochastic volatility." *Econometric Theory*, 34, 1207–1255. [1062]

Barndorff-Nielsen, Ole E., Peter Hansen, Asger Lunde, and Neil Shephard (2008), "Designing realized kernels to measure the ex-post variation of equity prices in the presence of noise." *Econometrica*, 76, 1481–1536. [1060]

Barndorff-Nielsen, Ole E. and Neil Shephard (2002), "Econometric analysis of realized volatility and its use in estimating stochastic volatility models." *Journal of the Royal Statistical Society Series B*, 64, 253–280. [1060]

Barndorff-Nielsen, Ole E. and Neil Shephard (2004a), "Econometric analysis of realised covariation: High frequency based covariance, regression and correlation in financial economics." *Econometrica*, 72, 885–925. [1060]

Barndorff-Nielsen, Ole E. and Neil Shephard (2004b), "Power and bipower variation with stochastic volatility and jumps." *Journal of Financial Econometrics*, 2, 1–37. [1060]

Bibinger, Markus, Nikolaus Hautsch, Peter Malec, and Markus Reiss (2019), "Estimating the spot covariation of asset prices – statistical theory and empirical evidence." *Journal of Business and Economic Statistics*, 37, 419–435. [1062]

Bollerslev, Tim, Andrew J. Patton, and Rogier Quaedvlieg (2016), "Exploiting the errors: A simple approach for improved volatility forecasting." *Journal of Econometrics*, 192, 1–18. [1090]

Campbell, John Y., Stefano Giglio, Christopher Polk, and Robert Turley (2018), "An intertemporal capm with stochastic volatility." *Journal of Financial Economics*, 128, 207–233. [1081, 1083, 1096]

Carrasco, Marine, Mikhail Chernov, Jean-Pierre Florens, and Eric Ghysels (2007), "Efficient estimation of general dynamic models with a continuum of moment conditions." *Journal of Econometrics*, 140, 529–573. [1075]

Casini, Alessandro and Pierre Perron (2019), "Continuous record Laplace-based inference about the break date in structural change models." Unpublished manuscript, Boston University. [1060]

Comte, Fabienne and Eric Renault (1998), "Long memory in continuous-time stochastic volatility models." *Mathematical Finance*, 8, 291–323. [1060, 1062]

Corsi, Fulvio (2009), "A simple approximate long-memory model of realized volatility." *Journal of Financial Econometrics*, 7, 174–196. [1092]

Dovonon, Prosper, Silvia Gonçalves, Ulrich Hounyo, and Nour Meddahi (2019), "Bootstrapping high-frequency jump tests." *Journal of the American Statistical Association*, 114, 793–803. [1061, 1062, 1066, 1067, 1068, 1069, 1071, 1072, 1082]

Engle, Robert F. (2004), "Risk and volatility: Econometric models and financial practice." *The American Economic Review*, 94, 405–420. [1060]

Foster, Dean P. and Daniel B. Nelson (1996), "Continuous record asymptotics for rolling sample variance estimators." *Econometrica*, 64 (1), 139–174. [1062]

Gonçalves, Silvia and Nour Meddahi (2009), "Bootstrapping realized volatility." *Econometrica*, 1, 283–306. [1061, 1062, 1065, 1069, 1081, 1082, 1097]

Hall, Peter (1992), *The Bootstrap and Edgeworth Expansion*. Springer, New York. [1070]

Hansen, Peter R., Asger Lunde, and James M. Nason (2011), "The model confidence set." *Econometrica*, 79, 453–497. [1092, 1095]

Hayashi, Takaki and Nakahiro Yoshida (2005), "On covariance estimation of non-synchronously observed diffusion processes." *Bernoulli*, 11, 359–379. [1060]

Hounyo, Ulrich (2017), "Bootstrapping integrated covariance matrix estimators in noisy jump-diffusion models with non-synchronous trading." *Journal of Econometrics*, 197, 130–152. [1062]

Hounyo, Ulrich (2019), "A local Gaussian bootstrap method for realized volatility and realized beta." *Econometric Theory*, 35, 360–416. [1062, 1066, 1067, 1068, 1069, 1079]

Hounyo, Ulrich, Silvia Gonçalves, and Nour Meddahi (2017), "Bootstrapping pre-averaged realized volatility under market microstructure noise." *Econometric Theory*, 33, 791–838. [1062]

Hounyo, Ulrich, Zhi Liu, and Rasmus T. Varneskov (2022), "A modified wild bootstrap procedure for Laplace transforms of volatility." Unpublished manuscript. https://papers.ssrn.com/sol3/papers.cfm?abstract_id=4187049. [1061, 1082]

Hounyo, Ulrich and Rasmus T. Varneskov (2017), "A local stable bootstrap for power variations of pure-jump semimartingales and activity index estimation." *Journal of Econometrics*, 198, 10–28. [1062]

Hounyo, Ulrich and Rasmus T. Varneskov (2020), "Inference for local distributions at high sampling frequencies: A bootstrap approach." *Journal of Econometrics*, 215, 1–34. [1068]

Hounyo, Ulrich, Zhi Liu, and Rasmus T. Varneskov (2023), "Supplement to 'Bootstrapping Laplace transforms of volatility'." *Quantitative Economics Supplemental Material*, 14, https://doi.org/10.3982/QE1929. [1063]

Jacod, Jean and Mathieu Rosenbaum (2013), "Quarticity and other functionals of volatility: Efficient estimation." *Annals of Statistics*, 41, 1462–1484. [1061, 1067]

Jacod, Jean and Mathieu Rosenbaum (2015), "Estimation of volatility functionals: The case of a $\sqrt{n}$ window." In *Large Deviations and Asymptotic Methods in Finance* (Peter K. Friz, Jim Gatheral, Archil Gulisashvili, Antoine Jacquier, and Josef Teichmann, eds.), 559–590, Springer, Cham. [1073]

Jacod, Jean and Viktor Todorov (2014), "Efficient estimation of integrated volatility in presence of infinite variation jumps." *Annals of Statistics*, 42, 1029–1069. [1072, 1073, 1074, 1075, 1076, 1077, 1082]

Jacod, Jean, Yingying Li, Per A. Mykland, Mark Podolskij, and Mathias Vetter (2009), "Microstructure noise in the continuous case: The pre-averaging approach." *Stochastic Processes and their Applications*, 119 (7), 2249–2276. [1060]

Jacod, Jean and Philip Protter (2012), *Discretization of Processes*. Springer, Berlin. [1067, 1072, 1073, 1074, 1075, 1076]

Jiang, George J. and John L. Knight (2002), "Estimation of cointinuous-time processes via empirical characteristic function." *Journal of Business and Economic Statistics*, 20, 198–212. [1075]

Kristensen, Dennis (2010), "Nonparametric filtering of the realized spot volatility: A kernel-based approach." *Econometric Theory*, 26, 60–93. [1062]

Lee, Suzanne S. and Per A. Mykland (2008), "Jumps in financial markets: A new nonparametric test and jump dynamics." *Review of Financial Studies*, 21, 2535–2563. [1061, 1062]

Li, Jia, Yunxiao Liu, and Dacheng Xiu (2019), "Efficient estimation of integrated volatility functionals via multiscale jackknife." *Annals of Statistics*, 47, 156–176. [1061]

Li, Jia, George Tauchen, and Viktor Todorov (2017), "Adaptive estimation of continuous-time regression models using high-frequency data." *Journal of Econometrics*, 200, 36–47. [1067]

Li, Jia, Viktor Todorov, and George Tauchen (2016), "Inference theory for volatility functional dependencies." *Journal of Econometrics*, 193, 17–34. [1061]

Li, Jia and Dacheng Xiu (2016), "Generalized method of integrated moments for high-frequency data." *Econometrica*, 84, 1613–1633. [1061, 1067]

Liu, Qiang, Yiqi Liu, and Zhi Liu (2018), "Estimating spot volatility in the presence of infinite variation jumps." *Stochastic Processes and their Applications*, 128 (6), 1958–1987. [1077]

Liu, Qiang and Zhi Liu (2020), "Statistical inference of spot correlation and spot market beta under infinite variation jumps." *Journal of Financial Econometrics*. (forthcoming). [1077]

Liu, Regina Y. (1988), "Bootstrap procedures under some non-i.i.d. models." *Annals of Statistics*, 16, 1696–1708. [1061, 1065, 1082, 1097, 1098]

Mancini, Cecilia (2009), "Non-parametric threshold estimation for models with stochastic diffusion coefficient and jumps." *Scandinavian Journal of Statistics*, 36, 270–296. [1060]

Podolskij, Mark and Daniel Ziggel (2010), "New tests for jumps in semimartingale models." *Statistical Inference for Stochastic Processes*, 13, 15–41. [1082]

Reiss, Markus, Viktor Todorov, and Geoge Tauchen (2015), "Nonparametric test for a constant beta between Itô semi-martingales based on high-frequency data." *Stochastic Processes and their Applications*, 125, 2955–2988. [1084]

Shao, Jun and Dongsheng Tu (1995), *The Jackknife and the Bootstrap*. Springer, New York. [1068]

Sims, Chris A. and Tao Zha (1999), "Error bands for impulse response functions." *Econometrica*, 67, 1113–1155. [1081]

Todorov, Viktor (2015), "Jump activity estimation for pure-jump semimartingales via self-normalized statistics." *Annals of Statistics*, 43, 1831–1864. [1060, 1082]

Todorov, Viktor, George Tauchen, and Iaryna Grynkiv (2011), "Realized Laplace transforms for estimation of jump diffusive volatility models." *Journal of Econometrics*, 164, 367–381. [1060, 1074]

Todorov, Viktor and George Tauchen (2012a), "Inverse realized Laplace transform for nonparametric volatility density estimation in jump diffusions." *Journal of the American Statistical Association*, 107, 622–635. [1060]

Todorov, Viktor and George Tauchen (2012b), "The realized Laplace transform of volatility." *Econometrica*, 80, 1105–1127. [1060, 1062, 1063, 1064]

Varneskov, Rasmus T. (2017), "Estimating the quadratic variation spectrum of noisy asset prices using generalized flat-top realized kernels." *Econometric Theory*, 33, 1457–1501. [1060]

Wang, Li, Zhi Liu, and Xiaochao Xia (2019), "Rate efficient estimation of realized Laplace transform of volatility with microstructure noise." *Scandinavian Journal of Statistics*, 46, 920–953. [1081]

Wu, Chen-Fu J. (1986), "Jackknife, bootstrap and other resampling methods in regression." *Annals of Statistics*, 14, 1261–1295. [1061, 1065, 1082, 1097, 1098]

Zhang, Lan, Per A. Mykland, and Yacine Aït-Sahalia (2005), "A tale of two time scales: Determining integrated volatility with noisy high frequency data." *Journal of the American Statistical Association*, 100, 1394–1411. [1060]

Zu, Yang and H. Peter Boswijk (2014), "Estimating spot volatility with high-frequency financial data." *Journal of Econometrics*, 181, 117–135. [1062]

Co-editor Tao Zha handled this manuscript.

Manuscript received 26 May, 2021; final version accepted 31 March, 2023; available online 21 April, 2023.